 doi:10.20944/preprints202208.0432.v1

Article

Multidecadal trend analysis of Armenian mountainous grassland and its relationship to climate change using multisensor NDVI time-series.

Vahagn Muradyan [1], Shushanik Asmaryan [1], Grigor Ayvazyan[1] and Fabio Dell'Acqua [2, *]

[1] Centre for Ecological-Noosphere Studies, National Academy of Sciences, Abovyan Street 68, Yerevan 0025, Armenia; vahagn.muradyan@cens.am (V. M.), shushanik.asmaryan@cens.am (Sh. A.), grigor.ayvazyan@cens.am (G. A.)

[2] University of Pavia, Department of Electrical, Computer and Biomedical Engineering, Via A. Ferrata 5, 27100, Pavia, Italy; fabio.dellacqua@unipv.it (F. D'A.)

* Correspondence: VM: vahagn.muradyan@cens.am; FD'A: fabio.dellacqua@unipv.it;

Abstract: This paper presents a comprehensive analysis of links between satellite-measured vegetation vigor and climate variables in Armenian mountain grassland ecosystems in years 1984–2018. NDVI is derived from MODIS and Landsat data, temperature and precipitation data are from meteorological stations. Two study sites were selected, representing arid and semi-arid grassland vegetation types, respectively. Various trend estimators including Mann-Kendall (MK) and derivatives were combined for vegetation change analysis at different time scales. Results suggest that temperature and precipitation had negative and positive impacts on vegetation growth, respectively, in both areas. NDVI-to-precipitation correlation was significant but with an apparent time-lag effect that was further investigated. No significant general changes were observed in vegetation along the observed period. Further comparisons between results from corrected and uncorrected data led us to conclude that MODIS and Landsat data with BRDF, topographic and atmospheric corrections applied are best suited for analyzing relationships between NDVI and climatic factors for the 2000-2018 period in grassland at a very local scale, but in the absence of correction tools and information, uncorrected data can still provide meaningful results. Future refinements will include removal of anthropogenic impact, and deeper investigation of time-lag effects of climatic factors on vegetation dynamics.

Keywords: NDVI, climatic factors, mountain grassland, time-lag effects, trends, Landsat, MODIS, BRDF, topographic and atmospheric corrections, Armenia

1. Introduction

Surface vegetation is one of the most important components of ecosystems on the Earth, playing a key role in regulating carbon balance and climate stability [1], [2], [3]. Vegetation is highly sensitive to climate change, particularly for that in mountain regions [4]. Mountain ecosystems are considered to be among those most severely and rapidly impacted by climate change [3], [4], [5], [6]. Thus, over the recent decades, monitoring vegetation dynamics and relationships with climate data have been recognized as a hot issue of global and regional change study, especially since satellite data started becoming increasingly available [9]–[12]. In order to comprehensively understand the impact of climatic factors on vegetation dynamics it is necessary to perform location-specific case studies on correlations between vegetation and climate factors in different geographical regions [6], [13]–[16].

 doi:10.20944/preprints202208.0432.v1

Remote sensing technologies as an alternative to time-consuming and labor-intensive field experimentation offer effective approaches that have been widely used to monitor surfaces vegetation dynamics in context of climate change [5], [15]–[18]. Remote sensing products such as Normalized Difference Vegetation Index (NDVI) are widely used to monitor the dynamics of vegetation in ecosystems and can be used as a proxy of vegetation response to climate change [10], [21]–[36]. In recent years, time-series NDVI datasets have been adopted to monitor vegetation dynamics and explore the relationship between NDVI and climate factors in different geographic regions [30], [37], [38]–[47] including both regional [14], [48], [49] and global scales [34], [50], [51]–[54].

The literature analysis shows that most of these studies were conducted on NDVI derived from satellite images at coarse spatial resolutions (NOAA/AVHRR, SPOT/VGT and MODIS) [11], [12], [14], [35], [38], [41], [44], [46], [51]–[57], which are inappropriate for resolving the local spatial variations. Satellite data at high temporal resolution are informative, but the coarse spatial resolution can suppress important changes at a very local scale. Moreover, MODIS and SPOT/VGT data only cover a limited time period (2000–2018) and may not be able to fully capture potential climate change impacts. On the contrary, the spatial resolution of the Landsat sensors is significantly finer and can cover a much longer time period (1984–2018), which facilitates detection of vegetation response to climate changes at a local scale [23], [31], [62], [63]. Most of previous studies widely used Landsat time series, which were focused on change detection and monitoring of vegetation [50], [64]–[67]. However, the use of Landsat time series to research on the relationships between vegetation and climate factors is limited [68].

Analyses of previous studies demonstrated that there was a similar performance of MODIS and Landsat data [69], [70]. Therefore, we can use the low spatial resolution MODIS data to study relationships between NDVI and climate factors [71].

Although the individual Landsat sensors have changed through time, the spectral characteristics from Landsat 4–8 are reasonably comparable and support the generation of dense time-series spectral information [31], [72]. However, Landsat satellite data received from different sensors need to be pre-processed, before drawing final conclusions about vegetation dynamics [73].

To get more accurate results usually Landsat and MODIS data are pre-processed using a number of methods: cloud masking, atmospheric correction, topographic correction, bidirectional reflectance distribution function (BRDF) correction [65], [74], [75]. BRDF correction with atmospheric correction is important for creating long-term time series of satellite data, and to allow comparison between measurements of NDVI from different sensors and times [76], [77]–[79], including both LANDSAT TM/ETM/ OLI [74], [75] and MODIS [80], [81].

Satellite surface reflectance values are adjusted to a nadir view and local solar observation geometry to provide nadir BRDF-adjusted surface reflectance data [82]. The BRDF correction method is used to correct differences in the field of view angles among satellites and the data received from different times of the same sensor, as the satellite orbit changes over time, and it can impact on NDVI values [83], [84]. In addition to the BRDF correction method, atmospheric and topographic corrections are also important. Atmospheric elements such as water vapor, total ozone column, and aerosol optical depth affect the accuracy of satellite-based NDVI data [85]. The differences in the NDVI values occur depending on the atmospheric correction method [86]. Topographic correction of satellite images over mountainous areas is very important [87], especially when the data are to be used for monitoring of surface vegetation [88], [89]. To our knowledge, only a few studies have reported the use of the BRDF, atmospheric and topographic corrected NDVI data with high spatial resolution in studying the impact of climate change on vegetation cover.

Many previous studies have reported strong correlations between NDVI and main climatic factors of precipitation and temperature [19], [90]–[93]. Furthermore, the relationships between climatic factors and NDVI/vegetation are different in various geographical

Preprints (www.preprints.org) | NOT PEER-REVIEWED | Posted: 25 August 2022 doi:10.20944/preprints202208.0432.v1

regions and types of land cover [44], [89], [94]. However, as a general pattern, precipitation is the climatic parameter less correlated with the NDVI. On the contrary, the most correlated climatic parameter is temperature [95].

During recent years, several studies have verified that the response of vegetation/NDVI to climatic factors feature obvious lag-time effects [26], [40], [48], [96]–[103], which indicates that vegetation growth may be primarily affected by past climate conditions. Furthermore, lag-time duration varied among climatic zones and land-cover types, generally the lag time of vegetation in arid areas is longer than that in humid areas [29], [48]. The same type of vegetation has different time-lag effects by different climatic factors, and different vegetation types respond differently to the same climatic factor [48], [96]. In the scientific literature, most previous studies on the time-lag responses were based on monthly or mean growing season NDVI data [6], [104], [105], which is not conducive to determining the lag. Therefore, in order to understand the dynamic of mountain ecosystems and their relationships with climatic factors, it is preferable to use 10-day time-lag data [106]. The information of the time-lag effects of climate change on NDVI is necessary to discover the mechanisms underlying climate vegetation relationships. Furthermore, it is necessary to take the time lag into consideration in grassland management strategies [107].

During the last decades, a number of studies have been implemented on climate change in Armenia and Caucasus. Most of these researches concerned the spatio-temporal trends of climate factors [25], [108]–[110]. Other studies investigated the impact of climate change on the ecosystems of Armenia [111]–[113] and Caucasus [63]. The previous study on the territory of Armenia concerned variations of NDVI and climatic factors; their relationships and lag-time effect using SPOT/VGT data with limited times series 1998-2013 and low spatial resolution. However, the time-lag effects are still poorly understood due to the focus on simultaneous climate conditions for the mountain ecosystem of Armenia. The studies of relationships between climatic factors and NDVI data derived from satellite images with high spatial resolution and with BRDF, atmospheric, topographic corrections in the local level in mountain regions is limited [89]. In order to understand the complex impact of climatic factors on surface vegetation dynamics, it is necessary to perform the study on a local scale.

Our study focuses on the grassland ecosystems, which is one of the most sensitive land cover types in mountain regions. Research on grassland carbon stocks in arid and semi-arid regions has attracted a great deal of attention in recent years [114], [115]. Grasslands are one of the most prevalent and widespread land cover vegetation types, covering more than a quarter of the global land area [116]. In mountainous regions, rural natural grassland ecosystems are highly sensitive to natural changes, and for that reason it is essential to monitor their dynamics in the context of climate change[18], [117], [118]. Remote sensing technologies are an effective tool to monitor grassland ecosystems from local to global scales [117], [119]. Grassland ecosystem dynamics reflects the global and regional scale of natural processes and local-scale anthropogenic changes [120]. However, two grassland areas with minimal anthropogenic impact were selected [121], in order to obtain the most realistic results for the relationships between climatic factors and natural vegetation changes.

The goal of this research was to study the time-lag effects of the vegetation responses to climate variables in the mountain grassland ecosystems during 1984–2018 using MODIS-, Landsat-derived NDVI data with BRDF, topographic and atmospheric corrections applied, temperature and precipitation data from meteorological stations and Google Earth Engine (GEE) cloud platform [122]. GEE is a cloud-based geospatial analysis platform for scientific analysis and visualization of geospatial datasets; it enables processing of satellite imagery to detect changes, which has been widely used in similar studies in recent years [37], [71], [123].

2. Materials and Methods

2.1. Study area

Preprints (www.preprints.org) | NOT PEER-REVIEWED | Posted: 25 August 2022 doi:10.20944/preprints202208.0432.v1

The Sisian study site (45°59'57.95"E, 39°31'57.55"N, 2000–1600 m above sea level) and the Meghri study site (46°16'23.77"E, 38°54'44.10"N, 1000–600 m above sea level), two typical arid and semi-arid grasslands on the Syunk administrative region near to meteorological stations, were selected as the study areas (Fig. 1). Sisian and Megri study sites are covered areas of around 200 ha, dominated by steppe grass and 400 ha, dominated by Mediterranean xerophytic grassland [124] respectively. The Syunik administrative region covers an area of some 4506 km2 in the southeast of Armenia and is characterized by specific natural and economic conditions. This region has a dry climate with an average annual temperature of 13.8°C. The spatial distribution of annual precipitation is quite irregular, and it may be hypothesized that such irregular distribution may have a role in reducing correlation with NDVI. The growing season period lasts from April to October [125].

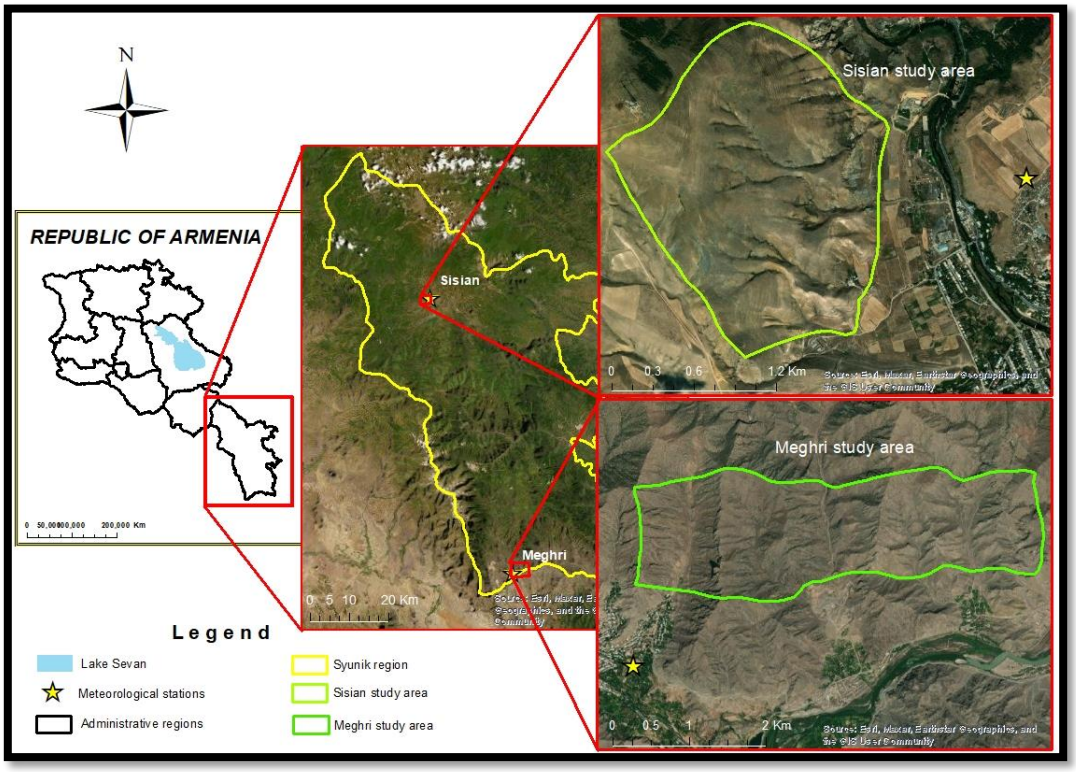

Figure 1. Study area

2.2. Data sources and processing

2.2.1 Data acquisition

In this paper, satellite and climatic data were used. Both datasets cover the period 1984–2018, whose length is defined by several factors. First, statistical analysis of trends in this context requires investigations over three decades at least [49]; second, satellite images with sufficiently high resolution must be available; and, finally, discovery of climatic trends needs long time spans. It was considered that climate warming generally intensified after the 1980–1990 decade both globally [126] and nationally [108]–[110].

2.2.1.1 Remote sensing data

The satellite data Landsat MSS/TM/ETM+/OLI Surface Reflectance Tier 1 and MODIS Nadir BRDF-Adjusted Reflectance, MODIS Surface Reflectance (SR) were accessed and processed for the intended 35 years through the Google Earth Engine (GEE) platform [122] using a JavaScript application programming interface (API). The MCD43A4 V6 Nadir Bidirectional Reflectance Distribution Function Adjusted Reflectance (NBAR) product

Preprints (www.preprints.org) | NOT PEER-REVIEWED | Posted: 25 August 2022 doi:10.20944/preprints202208.0432.v1

(MODIS/006/MCD43A4) provides reflectance data at 500-meter spatial resolution. Datasets are produced daily based on a 16-day retrieval period from both the Terra and Aqua spacecraft, choosing the best representative pixel from the 16-day period [122], [127]. The MOD09A1 V6.1 (MODIS/061/MOD09A1) product provides an estimate of the surface spectral reflectance of Terra MODIS at 500m resolution and is corrected for atmospheric conditions. In order to cover the 1984–2018 period, four collections of LANDSAT imagery were used: LANDSAT 5 MSS Surface Reflectance Tier 1 (LANDSAT/LM05/C01/T1_SR), for 1989, LANDSAT 5 TM Surface Reflectance Tier 1 (LANDSAT/LT05/C01/ T1_SR), for the period 1984–2011, LANDSAT 7 ETM + Surface Reflectance Tier 1 (LANDSAT/LE07/C01/T1_SR), for 1999–2018, and LANDSAT 8 OLI/TIRS (LANDSAT/LC08/C01/T1_SR), for 2013–2018 and MODIS for 2000-2018.

All these satellite data were downloaded for the vegetative period (from April to October) of each year. For the target period of 35 years, in the Sisian and Megri study cases a total of 1035 and 663 satellite images were used, respectively.

2.2.1.2 NDVI data computation

The NDVI values based on the red and near infrared bands were obtained from the MODIS and LANDSAT sensors for the two study areas corresponding to the vegetation period over 35 years (1984-2018) using a JavaScript API in GEE. Subsequently, 10-day (MODIS) and monthly (LANDSAT) NDVI images were derived by calculating the median NDVI value of all available scenes for the indicated time-period of each year. Median NDVI is less affected by outlier values [64]. Median seasons NDVI images from 1984 to 2018 were computed by averaging the monthly NDVI images of each year [18]. Then mean NDVI values from all grassland pixels within each study site were extracted for further analysis. During the analyses we considered an important fact, that Landsat OLI data are reported to have some differences when compared with previous Landsat sensors [50], [128], [129]. On average, the OLI TOA reflectance is greater than the ETM+ TOA reflectance for all bands, with greatest differences in the near-infrared. Therefore, it can also affect NDVI values. However, as shown in previous studies, the difference becomes smaller as NDVI increases [130]. Nevertheless, based on the transformation functions obtained from the previous studies, which were developed using ordinary least squares regression, the values of NDVI of Landsat 5/7 and 8 were normalized [129], [131].

2.2.1.3 Climate data

Daily meteorological data have been obtained from Armenia State Hydromet Service for two weather stations in study areas (Fig. 1). In order to study the relationship between the NDVI and climatic factors 10-day, monthly, seasonal (spring or April–May, summer or June–August and autumn or September–October)), humid period (April-June), dry period (July-August) sum precipitation and average temperature were calculated for the period from 1984 to 2018.

2.3. Method

2.3.1 Satellite data pre-processing

A series of image pre-processing steps, such as atmospheric, BRDF and topographic corrections, cloud and shadow masking were carried out to study vegetation change analysis using Landsat satellite data [50].

2.3.1.1 Atmospheric correction and cloud masking

Within the Google Earth Engine environment, all satellite images were corrected to surface reflectance using the LEDAPS method for Landsat MSS,TM, and ETM+ and the LaSRC method for Landsat OLI [64], [132]. For applying the cloud, shadow, water and snow masking to the LANDSAT MSS/TM–ETM /OLI images collection the necessary CFMASK algorithm, as well as a per-pixel saturation mask [133] were created by adapting the template provided by the GEE platform.

Preprints (www.preprints.org) | NOT PEER-REVIEWED | Posted: 25 August 2022 doi:10.20944/preprints202208.0432.v1

2.3.1.2 Topographic correction

Topographic correction of remote sensing data is required for mountainous terrain, because it accounts for variations in reflectance due to slope, aspect, and elevation [134]–[136]. The code of topographic correction in GEE was developed by [137] based on the modified Sun-Canopy-Sensor (SCS+C) topographic correction method [138]. These methods were applied for all Landsat images in the GEE environment.

2.3.1.3 BRDF effects correction

The Bidirectional Reflectance Distribution Functions (BRDF) model is applied to reduce the directional effects due to the differences in solar and view angles between Landsat sensors [78], [84], [131], [134]. As shown in some studies, Landsat 5 data may result in significant reflectance and NDVI differences due only to Landsat 5 orbit changes [140]. Moreover, Gao [141] and Roy [83] concluded that due to BRDF effects across the Landsat swath the red and NIR reflectance can vary by up to 0.02 and 0.06. Such angular effects can be corrected using a BRDF model. For the correction of BRDF effects from Landsat data, we used a semi-physical approach BRDF normalization proposed by Roy [83]. Regarding the MODIS NBAR (Nadir BRDF Adjusted Reflectance) imagery, they are provided to GEE [142]. The implementation of BRDF correction of Landsat images in GEE was developed by [137] based on Roy [83] algorithms.

2.3.2 Statistical analysis

Numerous methods have been adopted to estimate spatiotemporal vegetation changes and relationships between climatic factors, such as correlation and regression analysis, Sen and Mann Kendall models [82], [143], [144]. These methods have been validated for vegetation variation [82], [101], [143]. A Mann-Kendall test and Sen's slope method were used to estimate NDVI trends and the Pearson correlation method between NDVI and temperature and precipitation were computed to identify the role of climate factors in vegetation changes.

2.3.2.1 Trends analysis

To estimate the directional changes in NDVI time series, trend analysis were performed using data from different sensors [18], [45], [145]. Trend analysis was derived using the nonparametric original Mann-Kendall [146], [147], modified Mann-Kendall trend tests [148] and Sen's slope estimator [149], [150] all implemented based on the python package [151]. The advantage of Mann–Kendall is its suitability for small sample sizes and robustness against the effects of outliers [152]. However, the Mann-Kendall trend test is based on uncorrelated data, and test results tend to be affected by the persistence of time series [153], [154]. In order to reduce the impact of serial correlation on the Mann-Kendall test, Modified Mann-Kendall methods: pre-whitening; free pre-whitening; Hamed_Rao and Yue_Wang approaches [148], [152]–[155] were used. Modified Mann-Kendall methods were applied by many studies for NDVI long-time series trend analysis [45], [64].

The Kendall tau (τ) obtained from Mann-Kendell statistics was also used to measure the strength of the relationships. Mann–Kendall tau coefficient is ranged from −1 to 1, τ = 1 means a consistently increasing trend, while τ = −1 means a consistently decreasing trend, if τ= 0 means no trend exists. Significance of trend can be evaluated by using standardized z-score or p-value. A z-value ≥ 1.96 represents a statistically significant increase, while a z-value ≤−1.96 indicate significant decrease at the 95% (α = 0.5) significance level, if z-value is above or below 2.57 and -2,57 respectively, the trend in significant at 99% level [156], [157]. In this study, to test the significance of trends, as well as significance test was applied: strong significant ($p < 0.01$); significant ($0.01 < p < 0.05$); lower significant ($0.05 < p < 0.1$); insignificant level (p greater than 0.1) according to the F-test [158], [159].

In addition to the Mann-Kendall method, Sen's slope was also used to estimate the slope of NDVI. The Sen's slope estimation model [149] is suitable for the qualitative description of time series trends. Sen's slope is better for identifying the magnitude of the

 doi:10.20944/preprints202208.0432.v1

trend. If Sen's slope result is positive, the time series has an increasing trend; when the result is negative, the time series has a decreasing trend. In the last decades, it was widely applied in the studies of vegetation dynamics [14], [157].

2.3.2.2 Correlation and time-lag effects analysis

Pearson linear correlation coefficients (r) [160] were calculated to investigate temporal relationships between NDVI and precipitation and temperature across different time bases : spring, summer, autumn, dry period, humid period, months, 10-day periods respectively. The statistical significance of correlations was evaluated based on the t-test (at a significance level of 0.05 and 0.01). Moreover, the Pearson correlation was applied to analyze the lag-time effects between NDVI and climatic factors [43], [48], [101], [104], [161]. Considering that the influence of climate change on vegetation dynamics is a cumulative process [162] the response of vegetation growth to regular climatic factors (precipitation/temperature) in mountain ecosystems may have a time lag of 10 day, months and seasons (2-3 months) [15], [23], [26], [43], [48], [113], [163].

Thus, Pearson correlation analysis between 10-day, monthly, seasonally NDVI and average 10-day, monthly, seasonal temperature/precipitation during 1984–2018 growing season for two study areas were performed. All statistical correlation analysis was done using the R programming language.

3. Results and discussion

3.1. Relationships between NDVI and climate variables

3.1.1 Correlation and time-lag effects between MODIS NDVI data series and climatic factors

The correlations between the 10-day averaged climate data and NDVI values were assessed using MODIS data with BRDF and topographic, atmospheric corrections as well as MODIS Surface Reflectance data with only atmospheric correction. The latter will give an opportunity to understand the usefulness of applied preprocessing methods for the study of relationships. As can be seen from the tables of the two study areas (Sisian, Megri), a clear difference emerges between the correlation matrices with and without corrections. The correlation of climate data with the MODIS BRDF NDVI follows a regular pattern, in contrast to the MODIS SR NDVI, where the correlations seem to behave more randomly (Figure 2; Table 1, 2).

Considering the above-mentioned factors, we decided to opt for corrected rather than uncorrected data. Thus, in case of a large number of correlations, we discuss only those correlations between MODIS BRDF NDVI and climatic factors, which are statistically significant at the 0.05 and 0.01 level.

In the case of the Meghri arid study area, the correlation between NDVI and temperature/precipitation for the same 10-days is weak (Table 1) Instead, high correlations were found between NDVI and previous 10-day temperatures/precipitation. For instance, Table 2 shows that NDVI in 4th-6th and 13th-14th 10-days feature a significant negative correlation with temperature values in 3th and 12th 10-day periods, respectively. In the case of precipitation, there is a significant lag-time effect of 2nd, 3rd, 4rd, 5th, 6th,7th, 15th and 17th 10-day precipitation on NDVI values in 3th-6th, 6th-8th, 7th-8th, 8th-16th, 7th-19th, 15th-19th, 19th-21th 10-days respectively.

For the Sisian semi-arid area, an obvious lag-time effect of climatic factors on vegetation was observed, too (Figure 3, Table 3, 4). However, in contrast to Meghri, significant correlation was observed also for the same 10-days. For instance, NDVI in 4rd, 5th, 7th, 12th, 17th 10-days features a significant positive correlation with precipitation in the same 10-days whereas NDVI in 12th, 13th, 16th, 18th 10-days features a significant negative correlation with temperature in the same 10-day periods. Precipitation in 6th-8th,10th, 12th-13th,17th 10-days have a significant lag-time effect on 8th-11th, 8th-11th, 9th, 12th-13th, 13th-19th, 15th-19th, 18th-21st 10-day NDVI, respectively. Temperature also had a

 doi:10.20944/preprints202208.0432.v1

significant negative lag-time effect on NDVI, particularly in the case of 2nd, 7th, 12th-13th, 16th 10-days.

In summary, we may conclude that, in general, precipitation for the Meghri arid area had a lag-time effect, which started from the 1st 10-days, in contrast to the Sisian semi-arid area, where the lag-time effect is observed only from the 6th 10-days. The correlation between NDVI and temperature for the Meghri case is weak. However, the 6th, 7th, 12th, 17th 10-days have a significant lag-time effect on vegetation for both areas.

Preprints (www.preprints.org) | NOT PEER-REVIEWED | Posted: 25 August 2022 doi:10.20944/preprints202208.0432.v1

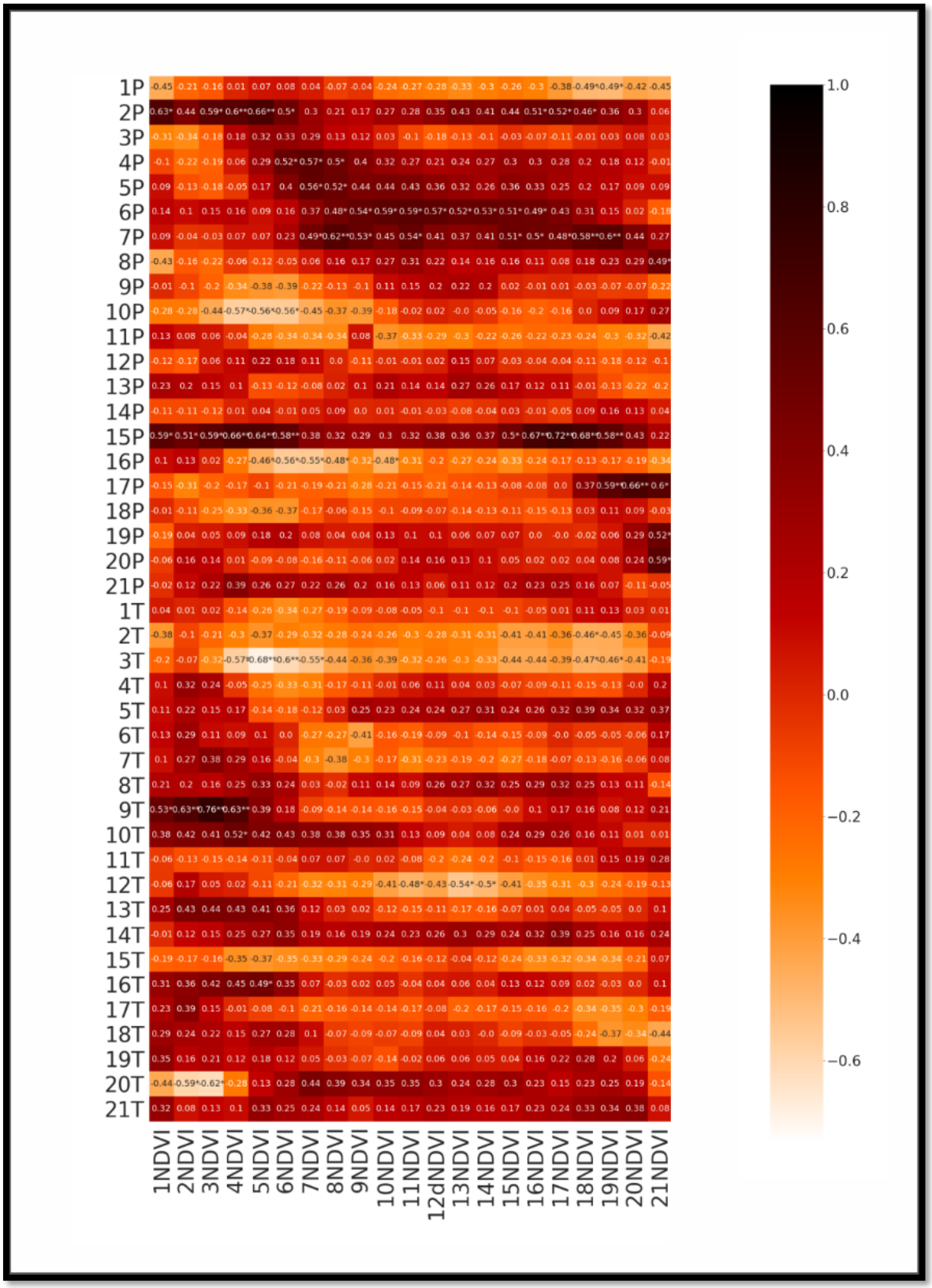

Figure 2. Correlation between 10-days values of temperature, precipitation and BRDF NDVI for Meghri, with the levels of significance: *- $p < 0.05$, ** $p < 0.01$

Preprints (www.preprints.org) | NOT PEER-REVIEWED | Posted: 25 August 2022 doi:10.20944/preprints202208.0432.v1

Table 1. The correlation between 10-days values of precipitation and SR NDVI for Meghri (*levels of significance: *- $p < 0.05$, ** $p < 0.01$*)

	1P	2P	3P	4P	5P	6P	7P	8P	9P	10P	11P	12P	13P	14P	15P	16P	17P	18P	19P	20P	21P
1NDVI	-.424																				
2NDVI	-.233	-.137																			
3NDVI	-.215	-.060	-.703**																		
4NDVI	-.468	.498*	-.462	-.034																	
5NDVI	-.230	.297	.377	-.048	.115																
6NDVI	-.068	-.044	.461	.722**	.644**	-.023															
7NDVI	.082	.390	.342	.115	.437	.464	-.157														
8NDVI	-.046	.152	.170	.454	.452	.444	.337	.159													
9NDVI	.236	.318	.316	.102	.304	.585*	.305	.175	-.233												
10NDVI	.061	.100	.209	.463	.456	.559*	.485*	.106	-.038	-.431											
11NDVI	-.230	-.025	.132	.284	.441	.543*	.487*	.355	.209	.179	-.180										
12dNDVI	.062	.017	.062	.122	.263	.315	.091	.355	-.266	-.158	-.148	-.274									
13NDVI	-.289	.552*	-.083	.288	.385	-.128	.158	-.164	-.251	-.171	-.179	.287	.192								
14NDVI	-.361	.069	-.063	.436	.420	.464	.529*	.293	-.021	-.155	-.143	-.008	.119	-.168							
15NDVI	-.106	.089	-.133	-.264	.154	.133	-.041	-.050	.261	.280	-.033	.309	.347	-.209	-.517*						
16NDVI	-.012	.527*	.380	.095	.215	.292	.153	.054	-.241	-.380	-.015	-.084	.260	.065	.332	-.545*					
17NDVI	-.125	.144	-.315	.145	.080	.211	-.038	.025	-.008	-.110	-.046	-.318	.272	-.118	.437	.000	-.573*				
18NDVI	-.349	.768**	.097	.072	.089	.366	-.246	-.408	.277	-.242	-.044	.285	.112	-.332	.375	-.077	-.035	-.448			
19NDVI	-.215	.083	-.235	.000	-.199	.027	.684**	.110	.193	.206	-.226	-.061	.260	.355	.050	.032	.401	.394	-.558*		
20NDVI	-.094	.235	.095	-.331	-.279	.257	.124	.140	.417	.392	.018	.052	-.243	.250	.147	.320	.590*	.380	-.242	-.090	
21NDVI	.157	.150	.254	.208	.245	.222	.201	.106	.147	-.029	-.011	.086	-.250	.315	-.149	-.197	.237	.055	.064	.009	-.542*

Preprints (www.preprints.org) | NOT PEER-REVIEWED | Posted: 25 August 2022 doi:10.20944/preprints202208.0432.v1

Table 2. The correlation between 10-days values of temperature and SR NDVI for Meghri (*levels of significance: *- p < 0.05, ** p < 0.01*)

	1T	2T	3T	4T	5T	6T	7T	8T	9T	10T	11T	12T	13T	14T	15T	16T	17T	18T	19T	20T	21T
1NDVI	.333																				
2NDVI	.034	.505*																			
3NDVI	.210	.240	.572*																		
4NDVI	-.022	-.309	-.183	.436																	
5NDVI	.487*	-.431	-.608**	-.428	.259																
6NDVI	-.211	.146	-.242	-.578*	-.161	-.035															
7NDVI	-.059	-.159	-.443	-.171	-.151	-.240	.248														
8NDVI	-.143	-.033	-.315	-.074	-.027	-.154	-.091	.397													
9NDVI	.060	-.361	-.568*	-.217	-.111	-.368	-.134	.104	.122												
10NDVI	-.049	-.260	-.381	-.323	-.098	-.414	-.310	-.030	-.266	.709**											
11NDVI	.098	-.179	-.202	-.166	.241	-.516*	-.283	-.053	-.160	.110	.437										
12dNDVI	-.124	.041	-.175	.044	-.081	.284	.084	.490*	.117	.460	-.056	.346									
13NDVI	-.278	-.309	-.276	.002	.073	.101	-.171	.063	.235	-.024	-.187	-.656**	.342								
14NDVI	-.096	.052	-.100	.013	.443	-.140	-.051	.167	.097	.336	-.086	-.266	.024	.627**							
15NDVI	.123	-.211	.048	.179	.133	-.230	-.302	-.352	-.342	-.572*	-.195	-.676**	-.380	-.239	.678**						
16NDVI	-.088	-.562*	-.688**	-.183	.073	-.291	-.131	.142	.163	.403	.229	-.382	-.030	-.082	-.232	.552*					
17NDVI	-.129	.120	.146	.057	.092	.415	.078	.520*	.137	.430	-.140	.164	.213	.382	-.210	.255	.615**				
18NDVI	.108	-.284	-.440	-.105	-.025	-.085	.349	.588*	.182	-.041	-.196	-.537*	-.040	.267	-.021	.337	-.259	.516*			
19NDVI	.216	-.395	-.142	-.153	.303	.070	-.430	-.258	-.351	-.147	-.045	-.213	-.281	-.216	-.244	-.416	-.303	-.601*	.318		
20NDVI	.274	-.412	-.342	.047	.113	-.323	.054	.069	.098	-.377	-.007	-.124	-.439	-.306	-.304	-.277	-.458	-.119	.359	.239	
21NDVI	-.358	-.427	-.468	.205	-.239	-.519*	-.358	-.029	-.346	-.102	.178	-.381	-.178	-.401	-.335	-.196	-.125	.203	-.019	.508*	.518*

Preprints (www.preprints.org) | NOT PEER-REVIEWED | Posted: 25 August 2022 doi:10.20944/preprints202208.0432.v1

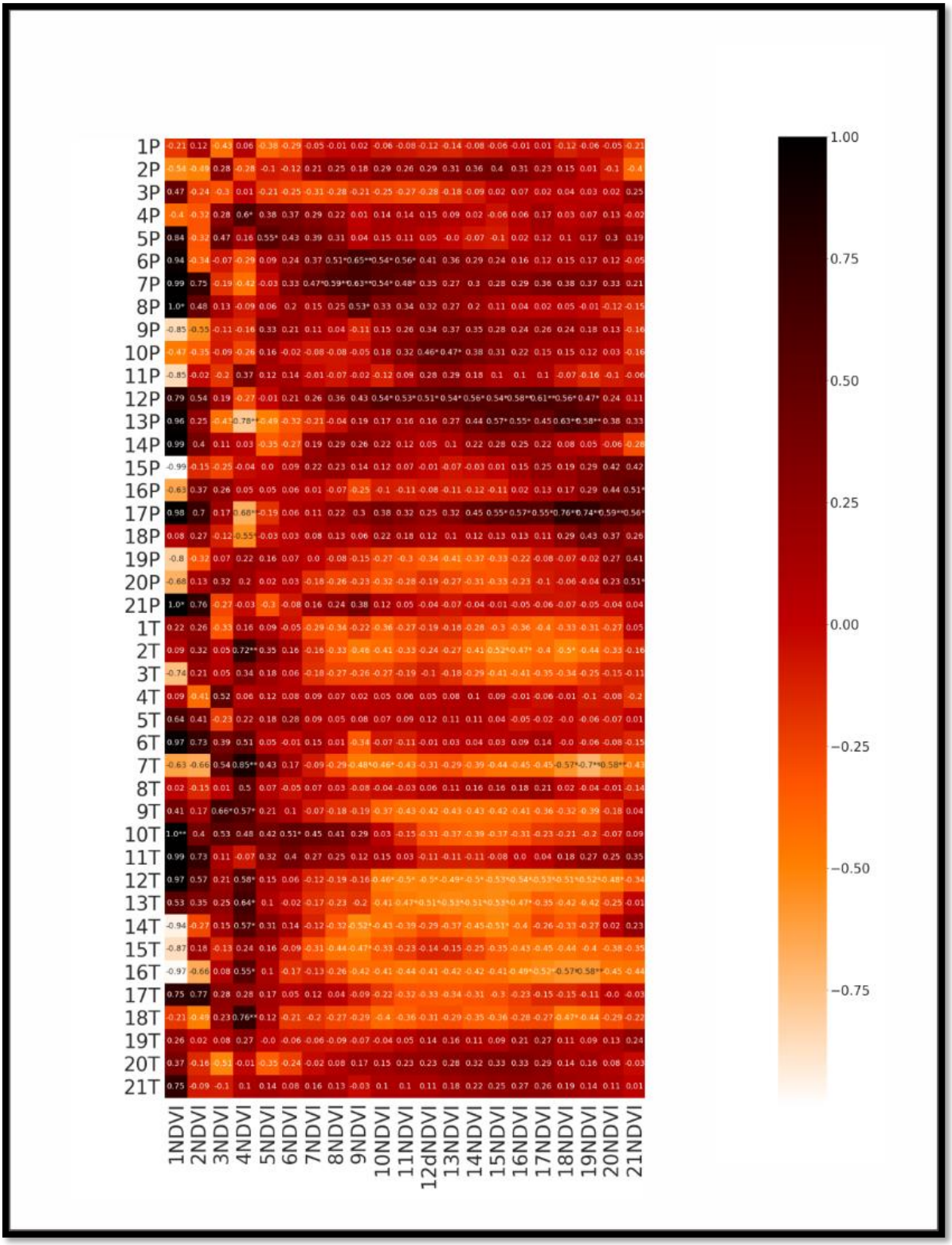

Figure 3. Correlation between 10-days values of temperature, precipitation and BRDF NDVI for Sisian, with the levels of significance: *- $p < 0.05$, ** $p < 0.01$

Preprints (www.preprints.org) | NOT PEER-REVIEWED | Posted: 25 August 2022 doi:10.20944/preprints202208.0432.v1

Table 3. The correlation between 10-days values of precipitation and SR NDVI for Sisian (*levels of significance: *- p < 0.05, ** p < 0.01*)

	1P	2P	3P	4P	5P	6P	7P	8P	9P	10P	11P	12P	13P	14P	15P	16P	17P	18P	19P	20P	21P
1NDVI	-.577*																				
2NDVI	-.250	-.587*																			
3NDVI	-.212	-.211	-.466																		
4NDVI	-.521*	.158	-.552*	-.270																	
5NDVI	-.461	-.124	.377	-.261	-.319																
6NDVI	.383	-.491*	-.030	.629**	.284	-.265															
7NDVI	-.553*	.036	.108	.041	-.018	.093	-.202														
8NDVI	.152	.055	-.181	.383	.435	.245	.065	-.477													
9NDVI	-.472	.409	.220	-.493	-.183	.325	.116	.085	-.084												
10NDVI	.238	.171	-.137	.264	.465	.465	.497*	.044	.119	.143											
11NDVI	-.163	-.059	.177	-.015	.147	.219	.106	.299	.437	.529*	-.116										
12dNDVI	.297	.133	-.198	.299	.311	.115	.152	-.352	.392	-.016	.548*	-.064									
13NDVI	-.202	.109	-.382	-.042	.270	.504*	.140	.367	.499*	.341	.221	.046	-.042								
14NDVI	-.298	.043	-.173	.266	.312	.144	-.062	.231	.736**	.701**	.501*	.240	-.169	-.313							
15NDVI	-.133	.325	-.352	-.418	-.187	.480	-.084	.474	.420	.647**	-.182	.055	.120	-.101	-.415						
16NDVI	.270	.529*	.359	-.288	-.291	-.014	.280	-.259	-.173	-.104	-.062	.062	.054	.415	.516*	-.545*					
17NDVI	.398	.255	-.387	.232	.340	-.201	.257	.068	.111	.117	.089	.180	-.424	.534*	.060	.419	-.407				
18NDVI	.093	.205	.156	.167	.390	.057	-.331	-.172	.388	.201	.477	-.122	-.221	.118	.243	-.048	-.312	-.543*			
19NDVI	-.115	.322	-.139	-.385	-.526*	-.087	.396	.414	.128	.176	-.063	.642**	.375	.209	-.398	-.212	.412	.055	-.444		
20NDVI	.015	.288	.189	.030	-.011	.157	.069	.083	.545*	.467	.178	.528*	.492*	-.001	-.087	-.366	.308	.090	-.314	-.592*	
21NDVI	-.020	.349	.111	.105	.397	.328	.042	-.152	.402	.308	-.186	.213	.328	.314	.089	.099	.267	.158	-.056	-.243	-.330

Preprints (www.preprints.org) | NOT PEER-REVIEWED | Posted: 25 August 2022 doi:10.20944/preprints202208.0432.v1

Table 4. The correlation between 10-days values of temperature and SR NDVI for Sisian (*levels of significance: *- p < 0.05, ** p < 0.01*)

	1T	2T	3T	4T	5T	6T	7T	8T	9T	10T	11T	12T	13T	14T	15T	16T	17T	18T	19T	20T	21T
1NDVI	.627**																				
2NDVI	.172	.508*																			
3NDVI	.277	.444	.690**																		
4NDVI	.145	-.123	.097	.345																	
5NDVI	.705**	.001	-.350	-.227	.478																
6NDVI	-.496*	.432	.361	-.227	.000	.213															
7NDVI	.575*	.240	-.095	-.021	.412	-.229	.706**														
8NDVI	-.015	.223	.039	.009	-.086	.083	.212	.461													
9NDVI	.216	-.438	-.595*	.285	.155	-.393	.264	-.154	.295												
10NDVI	-.148	-.211	-.187	-.297	-.264	-.394	-.450	-.074	-.637**	.245											
11NDVI	-.068	-.177	-.030	-.010	-.113	-.607**	-.328	-.361	-.181	-.308	.414										
12dNDVI	-.078	.183	.118	.123	-.248	.357	.127	.427	-.094	-.017	-.266	.187									
13NDVI	-.058	-.158	-.114	.049	.336	-.075	-.337	-.083	-.420	-.193	-.192	-.646**	-.313								
14NDVI	.167	.250	.213	.112	.113	-.072	.141	.251	-.124	-.289	-.128	-.203	-.113	.170							
15NDVI	.094	-.197	.035	.123	.000	-.088	-.294	-.464	-.423	-.684**	-.198	-.487*	-.622**	-.500*	.532*						
16NDVI	.052	-.515*	-.802**	-.307	.046	.168	-.038	.429	-.113	.069	.004	-.428	-.097	-.299	-.462	.364					
17NDVI	-.216	.212	.229	.031	-.248	.462	-.149	.293	-.233	.085	-.247	.092	.280	.064	-.077	-.161	.710**				
18NDVI	-.071	.055	-.256	.001	-.155	.120	.315	.458	.080	-.099	-.327	-.293	.118	.250	-.049	.244	.064	.576*			
19NDVI	.058	-.245	-.157	.097	.224	.298	-.229	-.070	-.247	-.317	-.122	-.041	-.114	-.568*	-.042	-.405	-.051	-.593*	-.149		
20NDVI	-.103	-.270	-.257	-.046	-.227	-.140	-.193	.096	-.411	-.459	.089	-.246	-.524*	-.638**	-.216	-.373	-.218	-.052	.036	.333	
21NDVI	-.452	-.372	-.349	.272	-.218	-.270	-.332	.204	-.286	-.145	-.083	-.565*	-.200	-.301	-.352	-.253	-.115	.002	-.102	.096	.110

 doi:10.20944/preprints202208.0432.v1

3.1.2 Correlation and Time-Lag effects between Landsat NDVI data series and climatic factors

To study relationships between climate factors and NDVI values, long time series (1984-2018) of Landsat data were considered. As the frequency of data acquisition for the Landsat sensor is lower (2-8 images per month), in this case the average monthly NDVI values were calculated. The response of NDVI to climate factors may differ according to vegetation type and growth phase [164] with obvious lag-time effect [15], [26], [104]. In some regions, NDVI variation is due to variation in precipitation [29], [102], [165]–[167] in other regions, temperature is a major influencing factor in the variation of NDVI [34], [46], [92], [93]. However, for the main cases of NDVI changes are dependent on both temperature and precipitation climatic factors [34], [59], [93], [168]. Therefore, to recognize seasonal differences and lag effects of climatic factors on NDVI within the growing season, we performed correlation analyses between seasonal mean NDVI and precipitation, temperature. The correlations were assessed using Landsat data with BRDF and topographic, atmospheric corrections as well as Landsat Surface Reflectance data with only atmospheric correction. As a result, for the two study areas (Sisian, Megri), there is a clear similarity between those two correlation matrices. Only a slight difference between the Megri area NDVI and temperature correlation matrices is observed. Therefore, it seems that both the Landsat BRDF-Adjusted Reflectance and Landsat Surface Reflectance data can be used to study the regularities of lag-time effect of monthly and seasonal precipitation/temperature on NDVI.

Figure 4, Table 5, 6 show that for the Meghri study area, summer and autumn NDVI feature significant positive correlation with spring and summer precipitation, respectively. Dry period NDVI significantly correlates with humid period precipitation and dry period temperature. For the Meghri arid area, a strong lag-time effect of climatic factors on vegetation was observed. In particular, NDVI of June-September, September, October significantly positively correlates with precipitation in May-June, August, September. For the Sisian semi-arid study area (Figure 5, Table 7, 8), summer and autumn NDVI correlated positively with summer precipitation and negatively with summer temperature. Dry period NDVI significantly correlated with both humid and dry period precipitation and temperature. As in the case of Megri, in the Sisian study NDVI of June-September significantly correlated with precipitation in May-June. However, correlation between NDVI and temperature is higher than in Meghri. There exists a significant lag-time effect of April-August temperature on June, July, August, September NDVI. The impact of the current month temperature on the NDVI was obvious in the case of April, August and September. In general, for arid and semi-arid study areas, NDVI correlated positively with precipitation and negatively with temperature. Meanwhile, the correlation between NDVI and precipitation was significant and showed strong lag effects.

Preprints (www.preprints.org) | NOT PEER-REVIEWED | Posted: 25 August 2022 doi:10.20944/preprints202208.0432.v1

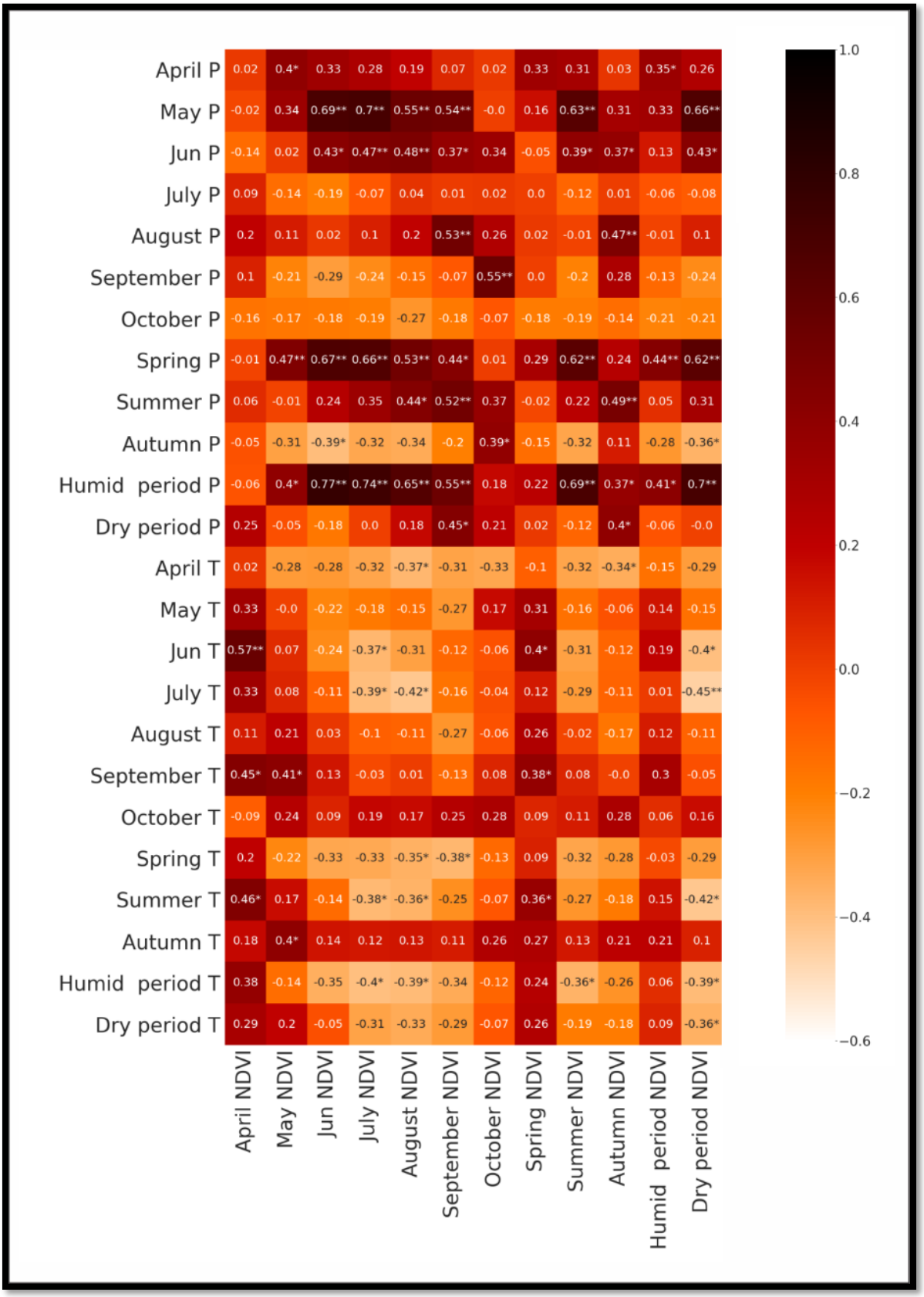

Figure 4. Correlation between averaged monthly and periodic values of temperature, precipitation and BRDF NDVI for Meghri, with the levels of significance: *- $p < 0.05$, ** $p < 0.01$

Preprints (www.preprints.org) | NOT PEER-REVIEWED | Posted: 25 August 2022 doi:10.20944/preprints202208.0432.v1

Table 5. Correlation between averaged monthly and periodic values of precipitation and SR NDVI for Meghri, with the levels of significance: *- p < 0.05, ** p < 0.01

	April P	May P	Jun P	July P	August P	September P	October P	Spring P	Summer P	Autum P	Humed period P	Dry period P
April NDVI	.072											
May NDVI	.564**	.354										
Jun NDVI	.399*	.667**	.455*									
July NDVI	.366*	.682**	.443**	-.151								
August NDVI	.306	.526**	.501**	-.021	.164							
September NDVI	.186	.532**	.488**	.034	.589**	-.082						
October NDVI	.078	.033	.369	-.018	.234	.550**	-.072					
Spring NDVI								.429*				
Summer NDVI								.668**	.305			
Autumn NDVI								.333	.581**	.086		
Humid period NDVI											.491**	
Dry period NDVI											.746**	-.013

Preprints (www.preprints.org) | NOT PEER-REVIEWED | Posted: 25 August 2022 doi:10.20944/preprints202208.0432.v1

Table 6. Correlation between averaged monthly and periodic values of temperature and SR NDVI for Meghri, with the levels of significance: *- p < 0.05, ** p < 0.01

	April T	May T	Jun T	July T	August T	Septem-ber T	October T	Spring T	Summer T	Autumn T	Humid period T	Dry period T
April NDVI	-.069											
May NDVI	-.432*	-.189										
Jun NDVI	-.344	-.305	-.300									
July NDVI	-.375*	-.314	-.475**	-.368*								
August NDVI	-.416*	-.246	-.352	-.375*	-.178							
September NDVI	-.353	-.336	-.208	-.244	-.399*	-.221						
October NDVI	-.384*	.112	-.156	.010	-.143	.044	.209					
Spring NDVI								-.003				
summer NDVI								-.437**	-.403*			
Autumn NDVI								-.373*	-.301	.116		
Humid period NDVI											-.062	
Dry period NDVI											-.496**	-.438**

Preprints (www.preprints.org) | NOT PEER-REVIEWED | Posted: 25 August 2022 doi:10.20944/preprints202208.0432.v1

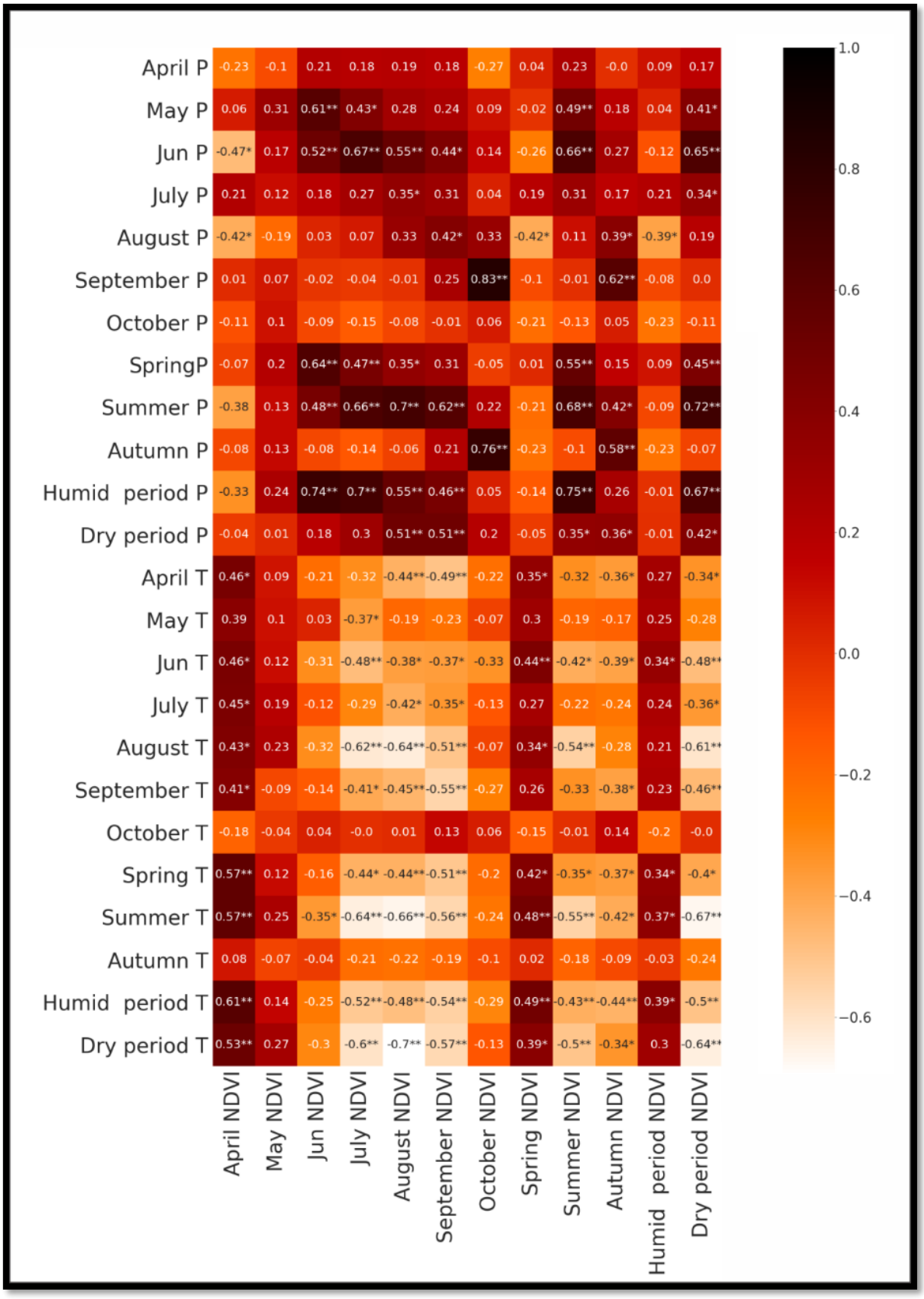

Figure 5. Correlation between averaged monthly and periodic values of temperature, precipitation and BRDF NDVI for Sisian, with the levels of significance: *- $p < 0.05$, ** $p < 0.01$

Preprints (www.preprints.org) | NOT PEER-REVIEWED | Posted: 25 August 2022 doi:10.20944/preprints202208.0432.v1

Table 7. Correlation between averaged monthly and periodic values of precipitation and SR NDVI for Sisian, with the levels of significance: *- p < 0.05, ** p < 0.01

	April P	May P	Jun P	July P	August P	September P	October P	Spring P	Summer P	Autumn P	Humid period P	Dry period P
April NDVI	-.188											
May NDVI	.076	.124										
Jun NDVI	.178	.534**	.557**									
July NDVI	.145	.396*	.643**	.287								
August NDVI	.193	.222	.519**	.342*	.367*							
September NDVI	.183	.242	.491**	.258	.414*	.256						
October NDVI	.029	-.020	.092	.081	.339	.768**	.003					
Spring NDVI								.189				
Summer NDVI								.513**	.663**			
Autumn NDVI								.178	.451**	.548**		
Humid period NDVI											.407*	
Dry period NDVI											.676**	.360*

Preprints (www.preprints.org) | NOT PEER-REVIEWED | Posted: 25 August 2022 doi:10.20944/preprints202208.0432.v1

Table 8. Correlation between averaged monthly and periodic values of temperature and SR NDVI for Meghri, with the levels of significance: *- p < 0.05, ** p < 0.01

	April T	May T	Jun T	July T	August T	September T	October T	Spring T	Summer T	Autumn T	Humid period T	Dry period T
April NDVI	.512*											
May NDVI	.124	.103										
Jun NDVI	-.269	.098	-.273									
July NDVI	-.320	-.357*	-.467**	-.301								
August NDVI	-.415*	-.096	-.276	-.414*	-.606**							
September NDVI	-.515**	-.275	-.431*	-.364*	-.515**	-.565**						
October NDVI	-.224	-.064	-.310	-.289	-.013	-.249	.240					
Spring NDVI								.217				
Summer NDVI								-.338*	-.511**			
Autumn NDVI								-.388*	-.440**	-.060		
Humid period NDVI											.072	
Dry period NDVI											-.492**	-.598**

 doi:10.20944/preprints202208.0432.v1

3.1.3 Comparison of Landsat- and MODIS-based products

Landsat and MODIS satellite images are used in various studies to analyze the relationship between vegetation of grasslands and climatic factors, as well as the time-lag effect. Therefore, it is necessary to compare the results obtained through those two sensors. For this purpose, the average monthly, seasonal Landsat/MODIS NDVI data (with BRDF and topographic, atmospheric correction) were calculated for the 2000-2018 period (Figure 6-9). The period 2000-2018 and monthly data were selected to provide comparability of MODIS and Landsat data.

As seen from the results, correlation matrices are similar in the two study areas. However, there are also some nuances; for instance, in the case of Meghri, strong correlation between Landsat NDVI (July, August) and June precipitation was observed, but MODIS NDVI significantly correlated with June precipitation only in July. For the Meghri arid area, correlation between both MODIS, Landsat NDVI and temperature is weak. For semi-arid grassland, the correlation matrices in case of precipitation are identical. A significant difference is observed only in the case of spring and summer temperature.

Summarizing the above-mentioned results, we can conclude that during study of relationships between NDVI and climatic factors for the 2000-2018 period in small grassland areas, both MODIS and Landsat BRDF-Adjusted satellite products are suitable.

Preprints (www.preprints.org) | NOT PEER-REVIEWED | Posted: 25 August 2022 doi:10.20944/preprints202208.0432.v1

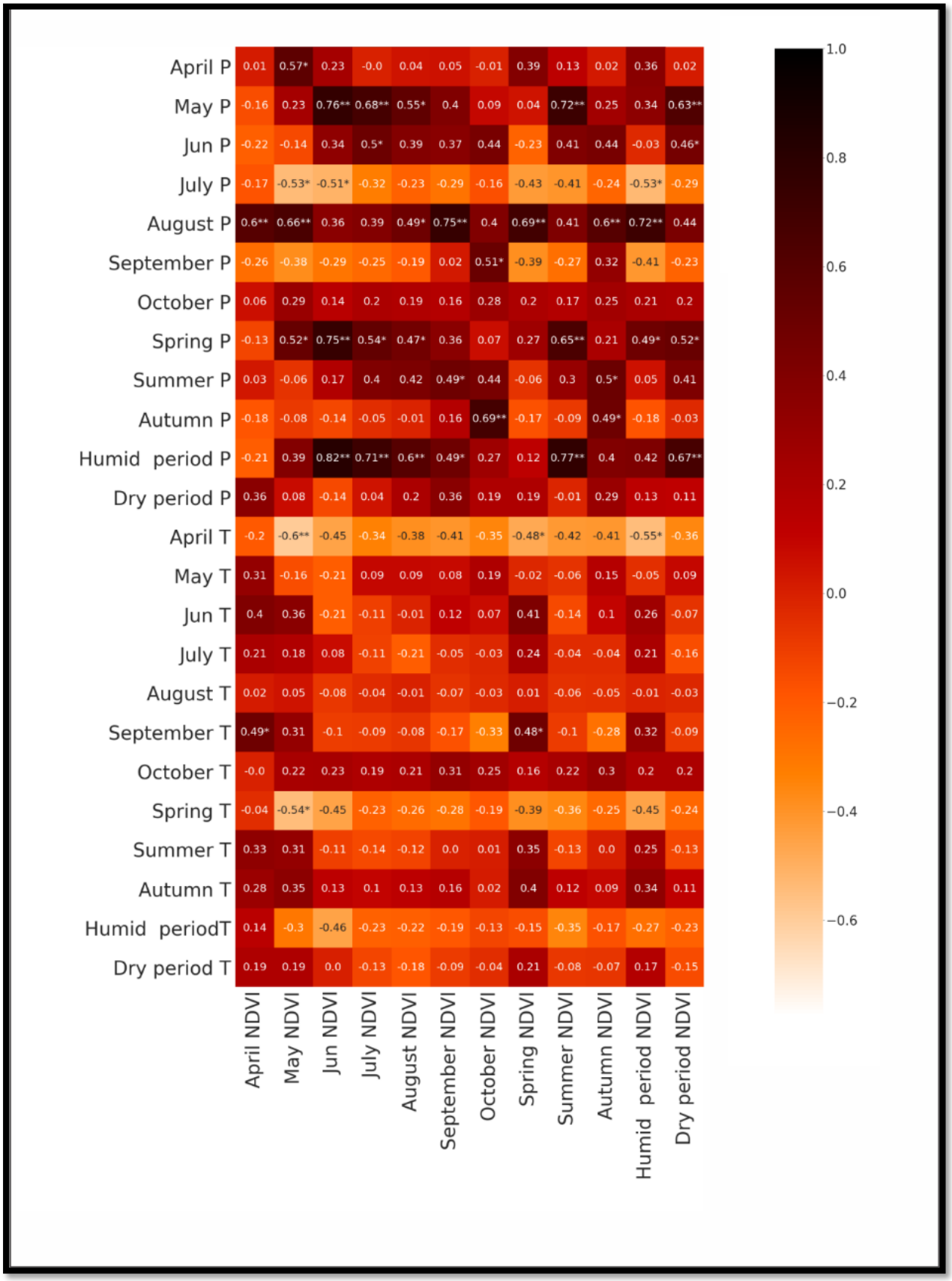

Figure 6. Correlation between temperature, precipitation and the average monthly, seasonal MODIS NDVI data (with BRDF and topographic, atmospheric correction) for Meghri for the 2000-2018 period.

Preprints (www.preprints.org) | NOT PEER-REVIEWED | Posted: 25 August 2022 doi:10.20944/preprints202208.0432.v1

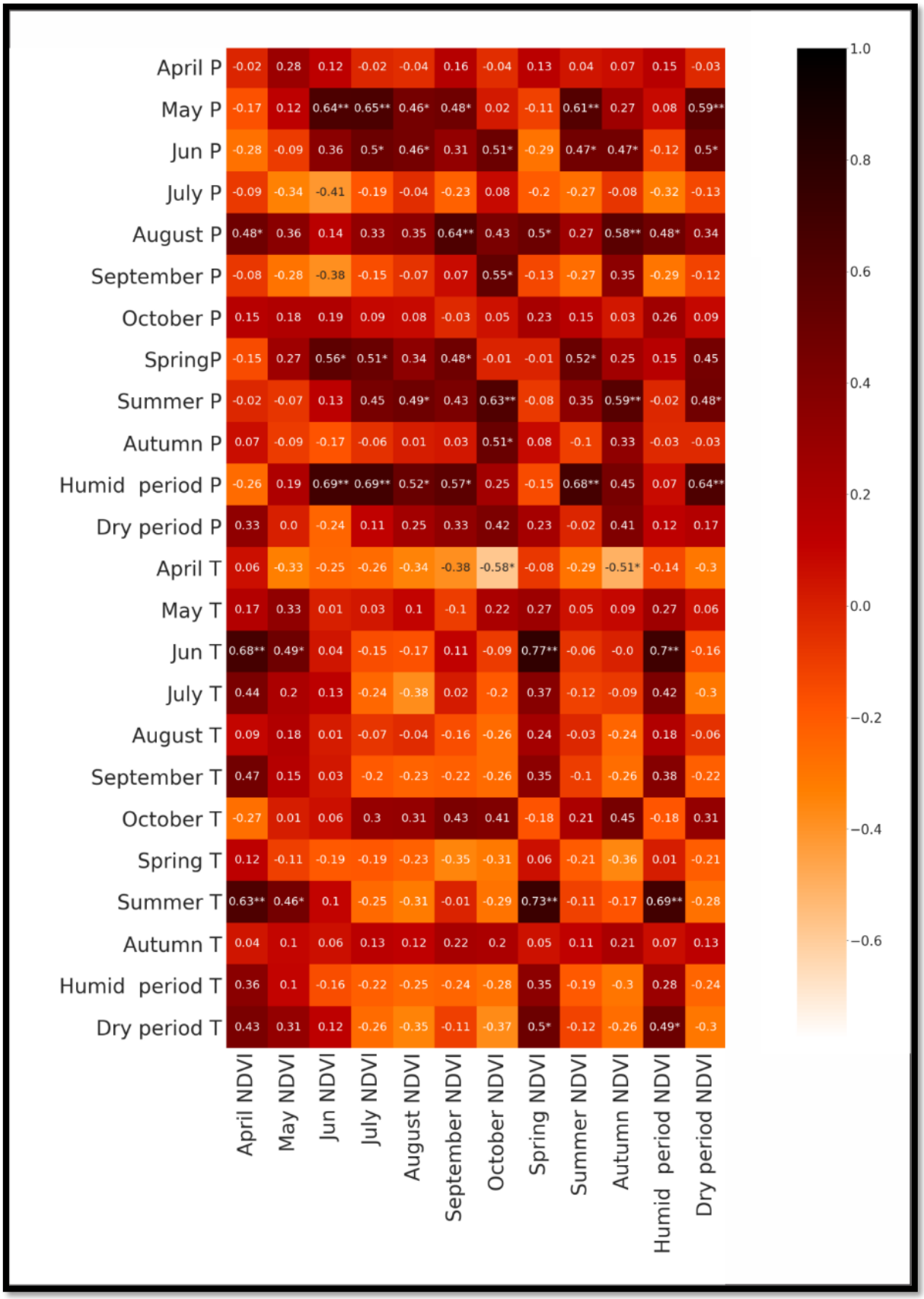

Figure 7. Correlation between temperature, precipitation and the average monthly, seasonal Landsat NDVI data (with BRDF and topographic, atmospheric correction) for Meghri for the 2000-2018 period.

Preprints (www.preprints.org) | NOT PEER-REVIEWED | Posted: 25 August 2022 doi:10.20944/preprints202208.0432.v1

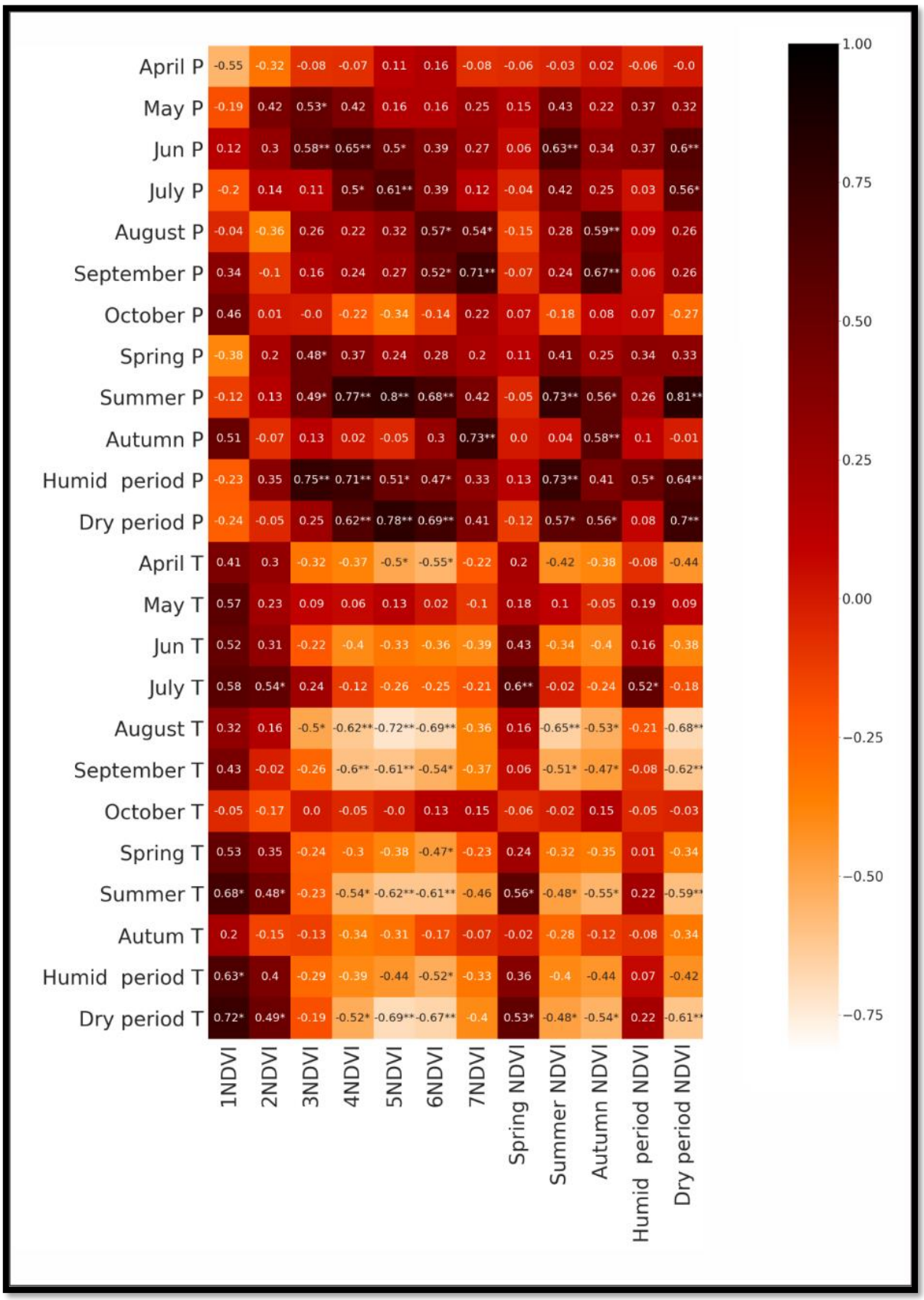

Figure 8. Correlation between temperature, precipitation and the average monthly, seasonal MODIS NDVI data (with BRDF and topographic, atmospheric correction) for Sisian for the 2000-2018 period.

Preprints (www.preprints.org) | NOT PEER-REVIEWED | Posted: 25 August 2022 doi:10.20944/preprints202208.0432.v1

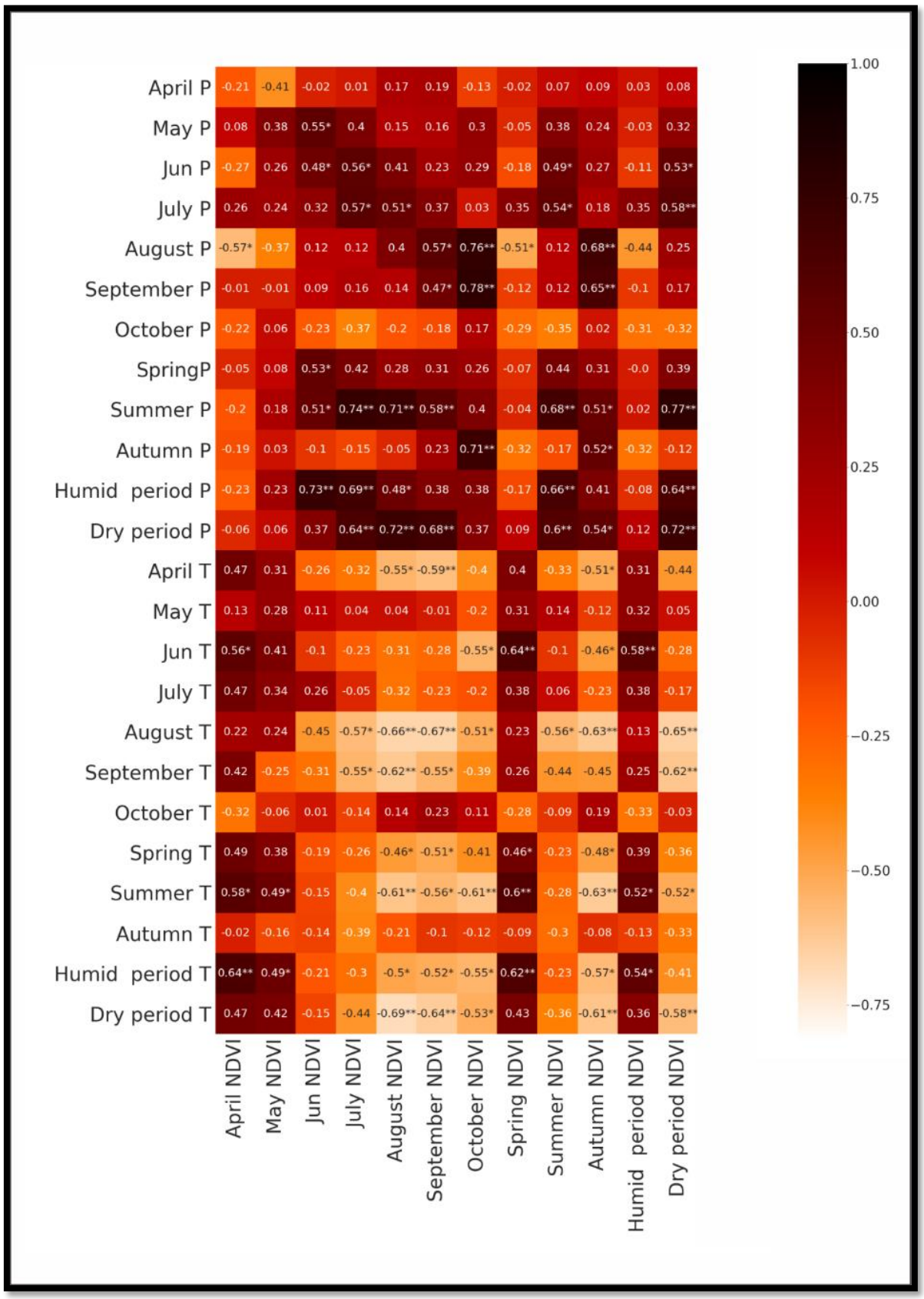

Figure 9. Correlation between temperature, precipitation and the average monthly, seasonal Landsat NDVI data (with BRDF and topographic, atmospheric correction) for Sisian for the 2000-2018 period.

 doi:10.20944/preprints202208.0432.v1

3.2 Spatiotemporal analyses of trend using Landsat NDVI time series

To analyze long-time spatiotemporal changes of vegetation of mountain grassland Landsat NDVI were used, which provide a long-time data series (1984-2018). Mann-Kendall (MK) and four modified Mann-Kendall methods (MMK) were applied to examine the trends. Previous studies showed better performance of the MMK method with the monthly data [169]. The results of the MK and MKK tests applied to the NDVI data series at a confidence interval of 90% are shown in Table 9. In an experiment reported in the scientific literature, the trend is considered significant only if at least three of the five tests suggest a significant trend [170]. In the same time, Sen's slope method was applied to discover trends in time series. The results were divided into a stable or no-trend region (−0.0005 < and ≤0.0005), an increasing region (> 0.0005), and a decreasing region (≤0.0005) [157].

Statistical results are shown in Table 9. Trend analysis indicated both significant increasing and no significant changes in monthly NDVI. In general, the results of test indicated a strong significant increasing trend in April, May NDVI at a confidence interval of 99% at the Meghri arid area (0.003, 0.002 year-1; respectively) and a no-trend or insignificant increasing/decreasing in all time periods NDVI at the Sisian semi-arid area. The MMK Yue-Wang test result at the Sisian area indicated a decreasing NDVI trend in September at a confidence interval of 95% (−0.0005 year-1), while the other Mann–Kendall tests did not indicate any significant trend. Also, a significant increase of mean spring, humid period NDVI during 1984–2018 was observed for Meghri arid area (Sen's slope = 0.002, and = 0.001; respectively). Trend analysis of monthly precipitation indicated no trend or insignificant changes at the both Sisian and Meghri study area. In contrast, the significant increase of temperature during 1984–2018 was detected. It is interesting to note that the Modified Mann-Kendall methods suggested by Yue and Wang [152] showed a significant trend in most of the cases as compared with other methods. The same situation was observed also in other investigations [170].

During the growing season the correlation between NDVI, and temperature and precipitation was negative and positive, respectively, indicating the positive effects of precipitation on vegetation growth, and negative effect of temperature, despite some shifts that were mainly insignificant. However, as shown in Figs. 2, 4, 6, 8 correlation between temperature and NDVI is lower than correlation between precipitation and NDVI, particularly at the Meghri arid study area, which was justified by some studies [102], [63], [168], [171]. It suggests that increasing temperature would not promote a decrease in vegetation. Considering the fact that precipitation has no trend, it can be justified that the NDVI of the two study areas was not changed in all months during 1984-2018, except for the spring months in Meghri arid area, where a significant increasing trend was recorded. The latter cannot be explained precisely by the available data; therefore, it is necessary to carry out additional analyses that include climatic factors of the previous months (February-March). Nevertheless, NDVI increased during spring and was stable during autumn, suggesting that the growing season may be starting earlier [14]. However, in general, no significant change in grassland vegetation has been recorded in the study area in the last three decades. In contrast, long-term positive changes in grassland vegetation (32.7% of grasslands) for the same period were found in the Caucasus region [63].

 doi:10.20944/preprints202208.0432.v1

Table 9. Trend analysis based on Landsat NDVI time series

Study area	Time series	MK			MMKH			MMKY			PW			TF PW			Sen's slope	Trend
		P	Z	Tau	P	Z	Tau	P	Z	Tau	P	Z	Tau	P	Z	Tau		
Meghri	*April*	0.04729	1.98374	0.28	0.00017	3.75712	0.28	0.000003	4.64521	0.28	0.07984	1.75162	0.25333	0.07212	1.79833	0.26	0.00372	Significant increasing
	May	0.01525	2.42638	0.31494	0.00153	2.42638	0.31494	0	8.44223	0.314943	0.07475	1.78201	0.23645	0.03733	2.08214	0.27586	0.00217	Significant increasing
	June	0.39559	0.84953	0.11640	0.23281	1.19314	0.11640	0.01227	2.50437	0.116402	0.80246	0.25016	0.03704	0.64650	0.45863	0.06553	0.00059	No trend
	July	0.59822	0.52697	0.06882	0.63648	0.47262	0.06882	0.13588	1.49131	0.068817	0.61739	0.49955	0.06667	0.54412	0.60659	0.08046	0.0004	No trend
	August	0.23415	1.18975	0.15269	0.10030	1.64338	0.15269	0.00125	3.22684	0.152688	0.47545	0.71364	0.09425	0.30077	1.03478	0.13563	0.00044	No trend
	September	0.29184	1.05408	0.13548	0.29185	1.05408	0.13548	0.00873	2.62261	0.135484	0.47545	0.71364	0.09425	0.47545	0.71364	0.09425	0.00033	No trend
	October	0.08958	1.69761	0.24	0.08958	1.69761	0.24	0.00007	3.98471	0.24	0.18311	0.33123	0.19333	0.12899	1.51807	0.22	0.00086	No trend
	Spring	0.01434	2.44868	0.30645	0.01434	2.44868	0.30645	0.0000003	5.07979	0.306452	0.01439	2.44748	0.31183	0.00531	2.78741	0.35484	0.00243	Significant increasing
	Summer	0.34458	0.94516	0.11742	0.17224	1.36503	0.11742	0.01651	2.39753	0.117424	0.88396	0.14595	0.02016	0.75799	0.30811	0.04032	0.00038	No trend
	Autumn	0.14003	1.47570	0.18548	0.14003	1.47570	0.18548	0.00101	3.28665	0.185484	0.39542	0.84982	0.10968	0.24778	2.52559	0.14839	0.00048	No trend
	Humid period	0.04378	2.01612	0.24421	0.04379	2.01612	0.24421	0.00002	4.20378	0.244207	0.02466	2.24669	0.27651	0.01155	1.05407	0.31061	0.00136	Significant increasing
	Dry period	0.49534	0.68184	0.08523	0.32516	0.98391	0.08523	0.08433	1.7261	0.085227	0.42684	0.79461	0.10081	0.29185	0.62035	0.13306	0.00040	No trend
Sisian	*April*	0.45961	0.73949	0.11463	0.45961	0.73949	0.11463	0.00874	2.622	0.114625	0.49856	0.67675	0.10822	0.53502	0.62035	0.09957	0.00259	No trend
	May	0.11012	1.59766	0.20430	0.02123	2.30384	0.20430	0.00008	3.94127	0.204301	0.16404	1.3916	0.18161	0.16404	1.3916	0.18161	0.00162	No trend
	June	0.26193	1.12176	0.14409	0.28225	1.07528	0.14409	0.00387	2.88878	0.144086	0.19895	1.28455	0.16782	0.09353	1.67706	0.21839	0.00175	No trend
	July	0.91363	-0.10850	-0.01515	0.91363	-0.10846	-0.01515	0.84126	-0.20028	-0.01515	0.98706	-0.01622	-0.00403	0.98706	-0.01622	-0.00403	-0.00014	No trend
	August	0.45856	-0.74122	-0.09091	0.45856	-0.74122	-0.09091	0.1628	-1.39556	-0.09091	0.63099	-0.48033	-0.06061	0.54566	-0.60428	-0.07576	-0.00007	No trend
	September	0.39008	-0.85947	-0.10887	0.39008	-0.85947	-0.10887	0.03963	-2.05756	-0.10887	0.61013	-0.50989	-0.06667	0.65856	-0.44191	-0.05806	-0.00058	No trend
	October	0.56090	0.5815	0.07882	0.12553	1.53196	0.07882	0.01061	2.55543	0.078818	0.51442	0.65196	0.08995	0.62137	0.49391	0.06898	0.00067	No trend
	Spring	0.22390	1.21623	0.15323	0.22390	1.21623	0.15323	0.00009	3.91593	0.153226	0.29198	1.05377	0.13548	0.41460	0.81583	0.10538	0.00145	No trend
	Summer	0.74432	0.32614	0.04099	0.74432	0.32614	0.04099	0.48019	0.70599	0.040998	0.88909	0.13945	0.01895	0.86466	0.17044	0.02273	0.00029	No trend
	Autumn	0.93825	-0.07747	-0.01136	0.88545	-0.14411	-0.01136	0.80212	-0.2506	-0.01136	0.78279	0.27568	0.03629	0.75799	0.30811	0.04032	-0.0001	No trend
	Humid period	0.14103	1.47197	0.18182	0.14103	1.47197	0.18182	0.00003	4.18204	0.181818	0.21179	1.24866	0.15726	0.22390	1.21623	0.15323	0.00161	No trend
	Dry period	0.78959	-0.26684	-0.03387	0.78959	-0.26684	-0.03387	0.57053	-0.56727	-0.03387	0.67569	0.41835	0.05303	0.72156	0.35637	0.04545	-0.00024	No trend

 doi:10.20944/preprints202208.0432.v1

4. Conclusions

This research analyzed temporal trends of MODIS, LANDSAT NDVI, climatic factors; studied the correlations and lag-time effects between grassland vegetation and climatic factors during the growing seasons (April–October) of the period 1984–2018 in Syunik region. For this purpose, 10-day, monthly, seasonal NDVI and precipitation, temperature data for two different study areas were used.

The results show that the correlation matrix of climate data with the MODIS BRDF NDVI follows a regular pattern, in contrast to the MODIS SR NDVI, where the correlations seem to behave more randomly. The results also confirm that for the Sisian and Megri study areas, there is a clear similarity between two correlation matrices: climatic data with Landsat BRDF; TC; AC NDVI, and climatic data with Landsat SR NDVI. It seems that both the Landsat BRDF:TC; AC and Landsat SR data can be used to study the regularities of lag-time effect of monthly and seasonal precipitation/temperature on NDVI.

The correlation between NDVI and climatic factors show that temperature had a negative impact and precipitation had positive impacts on vegetation growth in both arid and semi-arid areas. Meanwhile, the correlation between NDVI and precipitation was significant and has an apparent time-lag effect, yet a suitable time frame has to be selected for the phenomenon to become visible. In mountain arid and semi-arid grasslands, 10-day data are more suitable to understand the impact and lag-time effect of climatic factors on vegetation growth. For instance, the precipitation for the Meghri arid area had a lag-time effect, which is started from the 1st 10-days, in contrast to the Sisian semi-arid area, where the lag-time effect is observed only from the 6th 10-days. The correlation between NDVI and temperature for the Meghri case is weak. However, the 6th, 7th, 12th, 17th 10-days have a significant lag-time effect on vegetation for both areas.

Finally, we can conclude that for studying relationships between NDVI and climatic factors for the 2000-2018 period in grassland at a very local scale, both MODIS and Landsat BRDF-Adjusted satellite products are suitable.

In general, the analysis of changes of vegetation data for 45 years (1984-2018) of mountain grasslands showed no significant change of NDVI. However, other, more specific patterns have also been observed in the data. For example, a strong significant increasing trend in April, May NDVI at a confidence interval of 99% at the Meghri arid area (0.003, 0.002 year-1; respectively) and an insignificant increasing/decreasing in all time periods NDVI at the Sisian semi-arid area. The MMK Yue-Wang test result at the Sisian area indicated a decreasing NDVI trend in September at a confidence interval of 95% (−0.0005 year-1), while the other Mann–Kendall tests did not indicate any significant trend.

There are however other factors to consider, which will be incorporated in the future phases of our research. Last but not least, the effect of human activity on grasslands was not considered, although it surely has an impact on the evaluated variables. To refine the study, we will have to determine how to effectively remove anthropogenic impact, in order to establish a “cleaner” quantitative correlation between climatic factors and vegetation.

These results can assist to better understand the relations between NDVI and climatic factors, and may give guidance for the sustainable management of the mountain's grasslands by decision makers.

5. Patents

Not applicable.

Supplementary Materials: none.

Author Contributions: Conceptualization, V.M., Sh.A. and F.D'A. Methodology, V.M. and F.D'A. Data analysis and validation, V.M. and F.D'A. Writing—original draft preparation, V.M., G.A. and F.D'A. Writing—review and editing, V.M., Sh.A., G.A. and F.D'A. Visualization, V.M., G.A. and F.D'A. All authors have read and agreed to the published version of the manuscript.

Funding: The work was supported by the Science Committee of RA, in the framework of research project № 20TTCG-1E009.

Data Availability Statement: Not applicable

Acknowledgments: The authors wish to thank the University of Pavia for awarding a visiting grant to prof. Vahagn Muradyan in the framework of the CICOPS initiative. His visiting professor time in Pavia was extremely useful to advance the work described in this paper.

Conflicts of Interest: The authors declare no conflict of interest. The funders had no role in the design of the study; in the collection, analyses, or interpretation of data; in the writing of the manuscript; or in the decision to publish the results.

References

[1] W. Lucht *et al.*, "Climatic Control of the High-Latitude Vegetation Greening Trend and Pinatubo Effect," *Science*, vol. 296, no. 5573, pp. 1687–1689, May 2002, doi: 10.1126/science.1071828.

[2] G. Duveiller, J. Hooker, and A. Cescatti, "The mark of vegetation change on Earth's surface energy balance," *Nat Commun*, vol. 9, no. 1, Art. no. 1, Feb. 2018, doi: 10.1038/s41467-017-02810-8.

[3] X. Shen, B. Liu, D. Zhou, and X. Lu, "Effect of grassland vegetation on diurnal temperature range in China's temperate grassland region," *Ecological Engineering*, vol. 97, pp. 292–296, Dec. 2016, doi: 10.1016/j.ecoleng.2016.10.014.

[4] M. Wang, Z. Xiong, and X. Yan, "Modeling the climatic effects of the land use/cover change in eastern China," *Physics and Chemistry of the Earth, Parts A/B/C*, vol. 87–88, pp. 97–107, Jan. 2015, doi: 10.1016/j.pce.2015.07.009.

[5] M. Fort, "Impact of climate change on mountain environment dynamics," *Journal of Alpine Research | Revue de géographie alpine*, no. 103–2, Art. no. 103–2, Sep. 2015, doi: 10.4000/rga.2877.

[6] G. Hou, H. Zhang, and Y. Wang, "Vegetation dynamics and its relationship with climatic factors in the Changbai Mountain Natural Reserve," *J. Mt. Sci.*, vol. 8, no. 6, pp. 865–875, Dec. 2011, doi: 10.1007/s11629-011-2206-4.

[7] X. Liu, W. Zhou, and Z. Bai, "Vegetation coverage change and stability in large open-pit coal mine dumps in China during 1990–2015," *Ecological Engineering*, vol. 95, pp. 447–451, Oct. 2016, doi: 10.1016/j.ecoleng.2016.06.051.

[8] T. Schoolmeester *et al.*, *Outlook on climate change adaptation in the Tropical Andes mountains*. 2016. doi: 10.13140/RG.2.1.4311.1287.

[9] S. Piao *et al.*, "Altitude and temperature dependence of change in the spring vegetation green-up date from 1982 to 2006 in the Qinghai-Xizang Plateau," *Agricultural and Forest Meteorology*, vol. 151, no. 12, pp. 1599–1608, Dec. 2011, doi: 10.1016/j.agrformet.2011.06.016.

[10] N. Pan, X. Feng, B. Fu, S. Wang, F. Ji, and S. Pan, "Increasing global vegetation browning hidden in overall vegetation greening: Insights from time-varying trends," *Remote Sensing of Environment*, vol. 214, pp. 59–72, Sep. 2018, doi: 10.1016/j.rse.2018.05.018.

[11] A. Chen, B. He, H. Wang, L. Huang, Y. Zhu, and A. Lv, "Notable shifting in the responses of vegetation activity to climate change in China," *Physics and Chemistry of the Earth, Parts A/B/C*, vol. 87–88, pp. 60–66, Jan. 2015, doi: 10.1016/j.pce.2015.08.008.

[12] X. Guo, N. C. Coops, P. Tompalski, S. E. Nielsen, C. W. Bater, and J. John Stadt, "Regional mapping of vegetation structure for biodiversity monitoring using airborne lidar data," *Ecological Informatics*, vol. 38, pp. 50–61, Mar. 2017, doi: 10.1016/j.ecoinf.2017.01.005.

[13] B. Guo, Y. Zhou, S. Wang, and H. Tao, "The relationship between normalized difference vegetation index (NDVI) and climate factors in the semiarid region: A case study in Yalu Tsangpo River basin of Qinghai-Tibet Plateau," *J. Mt. Sci.*, vol. 11, no. 4, pp. 926–940, Jul. 2014, doi: 10.1007/s11629-013-2902-3.

[14] C. Li *et al.*, "Regional vegetation dynamics and its response to climate change—a case study in the Tao River Basin in Northwestern China," *Environ. Res. Lett.*, vol. 9, no. 12, p. 125003, Dec. 2014, doi: 10.1088/1748-9326/9/12/125003.

[15] V. Muradyan, G. Tepanosyan, S. Asmaryan, A. Saghatelyan, and F. Dell'Acqua, "Relationships between NDVI and climatic factors in mountain ecosystems: A case study of Armenia," *Remote Sensing Applications: Society and Environment*, vol. 14, pp. 158–169, Apr. 2019, doi: 10.1016/j.rsase.2019.03.004.

[16] H. Tang, Z. Li, Z. Zhu, B. Chen, B. Zhang, and X. Xin, "Variability and climate change trend in vegetation phenology of recent decades in the Greater Khingan Mountain area, Northeastern China," *Remote Sensing*, vol. 7, no. 9, Art. no. 9, Sep. 2015, doi: 10.3390/rs70911914.

[17] D. Pouliot, R. Latifovic, R. Fernandes, and I. Olthof, "Evaluation of annual forest disturbance monitoring using a static decision tree approach and 250 m MODIS data," *Remote Sensing of Environment*, vol. 113, no. 8, pp. 1749–1759, Aug. 2009, doi: 10.1016/j.rse.2009.04.008.

[18] Z. Li, T. Huffman, B. McConkey, and L. Townley-Smith, "Monitoring and modeling spatial and temporal patterns of grassland dynamics using time-series MODIS NDVI with climate and stocking data," *Remote Sensing of Environment*, vol. 138, pp. 232–244, Nov. 2013, doi: 10.1016/j.rse.2013.07.020.

[19] X. Wu *et al.*, "Normalized difference vegetation index dynamic and spatiotemporal distribution of migratory birds in the Poyang Lake wetland, China," *Ecological Indicators*, vol. 47, pp. 219–230, Dec. 2014, doi: 10.1016/j.ecolind.2014.01.041.

[20] L. Tong *et al.*, "Relative effects of climate variation and human activities on grassland dynamics in Africa from 2000 to 2015," *Ecological Informatics*, vol. 53, p. 100979, Sep. 2019, doi: 10.1016/j.ecoinf.2019.100979.

[21] W. Fang *et al.*, "Probabilistic assessment of remote sensing-based terrestrial vegetation vulnerability to drought stress of the Loess Plateau in China," *Remote Sensing of Environment*, vol. 232, p. 111290, Oct. 2019, doi: 10.1016/j.rse.2019.111290.

[22] M. Areola and M. Fasona, "Sensitivity of vegetation to annual rainfall variations over Nigeria," *Remote Sensing Applications: Society and Environment*, vol. 10, pp. 153–162, Apr. 2018, doi: 10.1016/j.rsase.2018.03.006.

[23] X. Jing, W.-Q. Yao, J.-H. Wang, and X.-Y. Song, "A study on the relationship between dynamic change of vegetation coverage and precipitation in Beijing's mountainous areas during the last 20 years," *Mathematical and Computer Modelling*, vol. 54, no. 3, pp. 1079–1085, Aug. 2011, doi: 10.1016/j.mcm.2010.11.038.

[24] V. Muradyan, S. Asmaryan, and A. Saghatelyan, "Assessment of space and time changes of NDVI (biomass) in Armenia's mountain ecosystems using remote sensing data," *Современные проблемы дистанционного зондирования Земли из космоса*, vol. 13, pp. 49–60, Jan. 2016, doi: 10.21046/2070-7401-2016-13-1-49-60.

[25] V. Muradyan, G. Tepanosyan, S. Asmaryan, and A. Sagharelyan, *Studying the dynamics of mountain ecosystems in the context of climate change employing remotely sensed data*. 2017. doi: 10.1117/12.2279423.

[26] J. Qi, S. Niu, Y. Zhao, M. Liang, L. Ma, and Y. Ding, "Responses of Vegetation Growth to Climatic Factors in Shule River Basin in Northwest China: A Panel Analysis," *Sustainability*, vol. 9, no. 3, Art. no. 3, Mar. 2017, doi:

10.3390/su9030368.

[27] S. Weishou, J. Di, Z. Hui, Y. Shouguang, L. Haidong, and L. Naifeng, "The Response Relation between Climate Change and NDVI over the Qinghai-Tibet plateau," *International Journal of Environmental and Ecological Engineering*, vol. 5, no. 11, pp. 761–767, Nov. 2011.

[28] Y. E. Yagoub *et al.*, "Correlation between Climate Factors and Vegetation Cover in Qinghai Province, China," *Journal of Geographic Information System*, vol. 9, no. 4, Art. no. 4, Jul. 2017, doi: 10.4236/jgis.2017.94025.

[29] W. Zhao, X. Zhao, T. Zhou, D. Wu, B. Tang, and H. Wei, "Climatic factors driving vegetation declines in the 2005 and 2010 Amazon droughts," *PLOS ONE*, vol. 12, no. 4, p. e0175379, Apr. 2017, doi: 10.1371/journal.pone.0175379.

[30] T. Na-U-Dom, X. Mo, and M. García, "Assessing the Climatic Effects on Vegetation Dynamics in the Mekong River Basin," *Environments*, vol. 4, no. 1, Art. no. 1, Mar. 2017, doi: 10.3390/environments4010017.

[31] H. James, V. LeMay, N. Coops, L. Verchot, P. Marshall, and K. Lochhead, "Canopy cover estimation in miombo woodlands of Zambia: Comparison of Landsat 8 OLI versus RapidEye imagery using parametric, nonparametric, and semiparametric methods," *Remote Sensing of Environment*, vol. 179, pp. 170–182, Jun. 2016, doi: 10.1016/j.rse.2016.03.028.

[32] L. Wang, X. Zhou, X. Zhu, Z. Dong, and W. Guo, "Estimation of biomass in wheat using random forest regression algorithm and remote sensing data," *The Crop Journal*, vol. 4, no. 3, pp. 212–219, Jun. 2016, doi: 10.1016/j.cj.2016.01.008.

[33] Z. Wen, S. Wu, J. Chen, and M. Lü, "NDVI indicated long-term interannual changes in vegetation activities and their responses to climatic and anthropogenic factors in the Three Gorges Reservoir Region, China," *Science of The Total Environment*, vol. 574, pp. 947–959, Jan. 2017, doi: 10.1016/j.scitotenv.2016.09.049.

[34] N. Linscheid *et al.*, "Towards a global understanding of vegetation–climate dynamics at multiple timescales," *Biogeosciences*, vol. 17, no. 4, pp. 945–962, Feb. 2020, doi: 10.5194/bg-17-945-2020.

[35] C. Zeng, H. Shen, and L. Zhang, "Recovering missing pixels for Landsat ETM+ SLC-off imagery using multi-temporal regression analysis and a regularization method," *Remote Sensing of Environment*, vol. 131, pp. 182–194, Apr. 2013, doi: 10.1016/j.rse.2012.12.012.

[36] P. Hawinkel, E. Swinnen, S. Lhermitte, B. Verbist, J. Van Orshoven, and B. Muys, "A time series processing tool to extract climate-driven interannual vegetation dynamics using Ensemble Empirical Mode Decomposition (EEMD)," *Remote Sensing of Environment*, vol. 169, pp. 375–389, Nov. 2015, doi: 10.1016/j.rse.2015.08.024.

[37] C. Liu *et al.*, "Quantitative spatial analysis of vegetation dynamics and potential driving factors in a typical alpine region on the northeastern Tibetan Plateau using the Google Earth Engine," *CATENA*, vol. 206, p. 105500, Nov. 2021, doi: 10.1016/j.catena.2021.105500.

[38] H. Chu, S. Venevsky, C. Wu, and M. Wang, "NDVI-based vegetation dynamics and its response to climate changes at Amur-Heilongjiang River Basin from 1982 to 2015," *Science of The Total Environment*, vol. 650, pp. 2051–2062, Feb. 2019, doi: 10.1016/j.scitotenv.2018.09.115.

[39] C. Ols, I. H. Kålås, I. Drobyshev, L. Söderström, and A. Hofgaard, "Spatiotemporal variation in the relationship between boreal forest productivity proxies and climate data," *Dendrochronologia*, vol. 58, p. 125648, Dec. 2019, doi: 10.1016/j.dendro.2019.125648.

[40] L. Zhao, Q. Li, Y. Zhang, H. Wang, and X. Du, "Normalized NDVI valley area index (NNVAI)-based framework for quantitative and timely monitoring of winter wheat frost damage on the Huang-Huai-Hai Plain, China," *Agriculture, Ecosystems & Environment*, vol. 292, p. 106793, Apr. 2020, doi: 10.1016/j.agee.2019.106793.

[41] L. Jiang, Y. Liu, S. Wu, and C. Yang, "Analyzing ecological environment change and associated driving factors in China based on NDVI time series data," *Ecological Indicators*, vol. 129, p. 107933, Oct. 2021, doi: 10.1016/j.ecolind.2021.107933.

[42] P. Li, J. Wang, M. Liu, Z. Xue, A. Bagherzadeh, and M. Liu, "Spatio-temporal variation characteristics of NDVI and its response to climate on the Loess Plateau from 1985 to 2015," *CATENA*, vol. 203, p. 105331, Aug. 2021, doi: 10.1016/j.catena.2021.105331.

[43] M. Zhe and X. Zhang, "Time-lag effects of NDVI responses to climate change in the Yamzhog Yumco Basin, South Tibet," *Ecological Indicators*, vol. 124, p. 107431, May 2021, doi: 10.1016/j.ecolind.2021.107431.

[44] M. Meng, N. Huang, M. Wu, J. Pei, J. Wang, and Z. Niu, "Vegetation change in response to climate factors and human activities on the Mongolian Plateau," *PeerJ*, vol. 7, p. e7735, Sep. 2019, doi: 10.7717/peerj.7735.

[45] Y. Li, Z. Xie, Y. Qin, and Z. Zheng, "Estimating Relations of Vegetation, Climate Change, and Human Activity: A Case Study in the 400 mm Annual Precipitation Fluctuation Zone, China," *Remote Sensing*, vol. 11, no. 10, Art. no. 10, Jan. 2019, doi: 10.3390/rs11101159.

[46] B. Baniya, Q. Tang, Z. Huang, S. Sun, and K. Techato, "Spatial and Temporal Variation of NDVI in Response to Climate Change and the Implication for Carbon Dynamics in Nepal," *Forests*, vol. 9, no. 6, Art. no. 6, Jun. 2018, doi: 10.3390/f9060329.

[47] X. Wang, Q. Gao, C. Wang, and M. Yu, "Spatiotemporal patterns of vegetation phenology change and relationships with climate in the two transects of East China," *Global Ecology and Conservation*, vol. 10, pp. 206–219, Apr. 2017, doi: 10.1016/j.gecco.2017.01.010.

[48] D. Wu *et al.*, "Time-lag effects of global vegetation responses to climate change," *Global Change Biology*, vol. 21, no. 9, pp. 3520–3531, 2015, doi: 10.1111/gcb.12945.

[49] R. Prăvălie *et al.*, "NDVI-based ecological dynamics of forest vegetation and its relationship to climate change in Romania during 1987–2018," *Ecological Indicators*, vol. 136, p. 108629, Mar. 2022, doi: 10.1016/j.ecolind.2022.108629.

[50] Z. Zhu, "Change detection using landsat time series: A review of frequencies, preprocessing, algorithms, and applications," *ISPRS Journal of Photogrammetry and Remote Sensing*, vol. 130, pp. 370–384, Aug. 2017, doi: 10.1016/j.isprsjprs.2017.06.013.

[51] Y. Julien, J. A. Sobrino, and J.-C. Jiménez-Muñoz, "Land use classification from multitemporal Landsat imagery using the Yearly Land Cover Dynamics (YLCD) method," *International Journal of Applied Earth Observation and Geoinformation*, vol. 13, no. 5, pp. 711–720, Oct. 2011, doi: 10.1016/j.jag.2011.05.008.

[52] C. Liu, X. Dong, and Y. Liu, "Changes of NPP and their relationship to climate factors based on the transformation of different scales in Gansu, China," *CATENA*, vol. 125, pp. 190–199, Feb. 2015, doi: 10.1016/j.catena.2014.10.027.

[53] F. Tian, R. Fensholt, J. Verbesselt, K. Grogan, S. Horion, and Y. Wang, "Evaluating temporal consistency of long-term global NDVI datasets for trend analysis," *Remote Sensing of Environment*, vol. 163, pp. 326–340, Jun. 2015, doi: 10.1016/j.rse.2015.03.031.

[54] Z. Yang, W. Li, X. Li, and J. He, "Quantitative analysis of the relationship between vegetation and groundwater buried depth: A case study of a coal mine district in Western China," *Ecological Indicators*, vol. 102, pp. 770–782, Jul. 2019, doi: 10.1016/j.ecolind.2019.03.027.

[55] R. Fensholt and I. Sandholt, "Evaluation of MODIS and NOAA AVHRR vegetation indices with in situ measurements in a semi-arid environment," *International Journal of Remote Sensing*, vol. 26, no. 12, pp. 2561–2594, Jun. 2005, doi: 10.1080/01431160500033724.

[56] R. Fensholt, I. Sandholt, M. S. Rasmussen, S. Stisen, and A. Diouf, "Evaluation of satellite based primary production modelling in the semi-arid Sahel," *Remote Sensing of Environment*, vol. 105, no. 3, pp. 173–188, Dec. 2006, doi: 10.1016/j.rse.2006.06.011.

[57] L. Liu *et al.*, "Evaluating the potential of MODIS satellite data to track temporal dynamics of autumn phenology in a temperate mixed forest," *Remote Sensing of Environment*, vol. 160, pp. 156–165, Apr. 2015, doi:

10.1016/j.rse.2015.01.011.

[58] B. J.-B. Zoungrana, C. Conrad, M. Thiel, L. K. Amekudzi, and E. D. Da, "MODIS NDVI trends and fractional land cover change for improved assessments of vegetation degradation in Burkina Faso, West Africa," *Journal of Arid Environments*, vol. 153, pp. 66–75, Jun. 2018, doi: 10.1016/j.jaridenv.2018.01.005.

[59] D. Mao, Z. Wang, L. Luo, and C. Ren, "Integrating AVHRR and MODIS data to monitor NDVI changes and their relationships with climatic parameters in Northeast China," *International Journal of Applied Earth Observation and Geoinformation*, vol. 18, pp. 528–536, Aug. 2012, doi: 10.1016/j.jag.2011.10.007.

[60] A. Chakraborty, M. V. R. Seshasai, C. S. Reddy, and V. K. Dadhwal, "Persistent negative changes in seasonal greenness over different forest types of India using MODIS time series NDVI data (2001–2014)," *Ecological Indicators*, vol. 85, pp. 887–903, Feb. 2018, doi: 10.1016/j.ecolind.2017.11.032.

[61] X. Fan, Y. Liu, J. Tao, Y. Wang, and H. Zhou, "MODIS detection of vegetation changes and investigation of causal factors in Poyang Lake basin, China for 2001–2015," *Ecological Indicators*, vol. 91, pp. 511–522, Aug. 2018, doi: 10.1016/j.ecolind.2018.04.041.

[62] P. Griffiths, C. Nendel, J. Pickert, and P. Hostert, "Towards national-scale characterization of grassland use intensity from integrated Sentinel-2 and Landsat time series," *Remote Sensing of Environment*, vol. 238, p. 111124, Mar. 2020, doi: 10.1016/j.rse.2019.03.017.

[63] K. E. Lewińska *et al.*, "Changes in the grasslands of the Caucasus based on Cumulative Endmember Fractions from the full 1987–2019 Landsat record," *Science of Remote Sensing*, vol. 4, p. 100035, Dec. 2021, doi: 10.1016/j.srs.2021.100035.

[64] F. E. Fassnacht, C. Schiller, T. Kattenborn, X. Zhao, and J. Qu, "A Landsat-based vegetation trend product of the Tibetan Plateau for the time-period 1990–2018," *Sci Data*, vol. 6, no. 1, Art. no. 1, May 2019, doi: 10.1038/s41597-019-0075-9.

[65] S. Qiu, Y. Lin, R. Shang, J. Zhang, L. Ma, and Z. Zhu, "Making Landsat Time Series Consistent: Evaluating and Improving Landsat Analysis Ready Data," *Remote Sensing*, vol. 11, no. 1, Art. no. 1, Jan. 2019, doi: 10.3390/rs11010051.

[66] J. E. Vogelmann, G. Xian, C. Homer, and B. Tolk, "Monitoring gradual ecosystem change using Landsat time series analyses: Case studies in selected forest and rangeland ecosystems," *Remote Sensing of Environment*, vol. 122, pp. 92–105, Jul. 2012, doi: 10.1016/j.rse.2011.06.027.

[67] M. C. Hansen *et al.*, "Monitoring conterminous United States (CONUS) land cover change with Web-Enabled Landsat Data (WELD)," *Remote Sensing of Environment*, vol. 140, pp. 466–484, Jan. 2014, doi: 10.1016/j.rse.2013.08.014.

[68] K. Zheng, J.-S. Ye, B.-C. Jin, F. Zhang, J.-Z. Wei, and F.-M. Li, "Effects of agriculture, climate, and policy on NDVI change in a semi-arid river basin of the Chinese Loess Plateau," *Arid Land Research and Management*, vol. 33, no. 3, pp. 321–338, Jul. 2019, doi: 10.1080/15324982.2018.1555562.

[69] R. Albarakat and V. Lakshmi, "Comparison of Normalized Difference Vegetation Index Derived from Landsat, MODIS, and AVHRR for the Mesopotamian Marshes Between 2002 and 2018," *Remote Sensing*, vol. 11, no. 10, Art. no. 10, Jan. 2019, doi: 10.3390/rs11101245.

[70] G. Wang, J. Wang, X. Zou, G. Chai, M. Wu, and Z. Wang, "Estimating the fractional cover of photosynthetic vegetation, non-photosynthetic vegetation and bare soil from MODIS data: Assessing the applicability of the NDVI-DFI model in the typical Xilingol grasslands," *International Journal of Applied Earth Observation and Geoinformation*, vol. 76, pp. 154–166, Apr. 2019, doi: 10.1016/j.jag.2018.11.006.

[71] Benedict and L. M. Jaelani, "A Long-term Spatial and Temporal Analysis of NDVI Changes in Java Island Using Google Earth Engine," *IOP Conf. Ser.: Earth Environ. Sci.*, vol. 936, no. 1, p. 012038, Dec. 2021, doi: 10.1088/1755-1315/936/1/012038.

[72] B. L. Markham and D. L. Helder, "Forty-year calibrated record of earth-reflected radiance from Landsat: A review," *Remote Sensing of Environment*, vol. 122, pp. 30–40, Jul. 2012, doi: 10.1016/j.rse.2011.06.026.

[73] S. Arjasakusuma, Y. Yamaguchi, T. Nakaji, Y. Kosugi, S.-A. Shamsuddin, and M. Lion, "Assessment of values and trends in coarse spatial resolution NDVI datasets in Southeast Asia landscapes," *European Journal of Remote Sensing*, vol. 51, no. 1, pp. 863–877, Jan. 2018, doi: 10.1080/22797254.2018.1496799.

[74] J. Barnetson, S. Phinn, P. Scarth, and R. Denham, "ASSESSING LANDSAT FRACTIONAL GROUND-COVER TIME SERIES ACROSS AUSTRALIA'S ARID RANGELANDS: SEPARATING GRAZING IMPACTS FROM CLIMATE VARIABILITY," in *The International Archives of the Photogrammetry, Remote Sensing and Spatial Information Sciences*, Nov. 2017, vol. XLII-3-W2, pp. 15–26. doi: 10.5194/isprs-archives-XLII-3-W2-15-2017.

[75] F. Li *et al.*, "Improving BRDF normalisation for Landsat data using statistical relationships between MODIS BRDF shape and vegetation structure in the Australian continent," *Remote Sensing of Environment*, vol. 195, pp. 275–296, Jun. 2017, doi: 10.1016/j.rse.2017.03.032.

[76] N.-H. Seong, D. Jung, J. Kim, and K.-S. Han, "Evaluation of NDVI Estimation Considering Atmospheric and BRDF Correction through Himawari-8/AHI," *Asia-Pacific J Atmos Sci*, vol. 56, no. 2, pp. 265–274, May 2020, doi: 10.1007/s13143-019-00167-0.

[77] J. León-Tavares, J.-L. Roujean, B. Smets, E. Wolters, C. Toté, and E. Swinnen, "Correction of Directional Effects in VEGETATION NDVI Time-Series," *Remote Sensing*, vol. 13, no. 6, Art. no. 6, Jan. 2021, doi: 10.3390/rs13061130.

[78] M. Buchhorn, M. K. Raynolds, and D. A. Walker, "Influence of BRDF on NDVI and biomass estimations of Alaska Arctic tundra," *Environ. Res. Lett.*, vol. 11, no. 12, p. 125002, Nov. 2016, doi: 10.1088/1748-9326/11/12/125002.

[79] B. Franch *et al.*, "A Method for Landsat and Sentinel 2 (HLS) BRDF Normalization," *Remote Sensing*, vol. 11, no. 6, Art. no. 6, Jan. 2019, doi: 10.3390/rs11060632.

[80] C. A. Petri and L. S. Galvão, "Sensitivity of Seven MODIS Vegetation Indices to BRDF Effects during the Amazonian Dry Season," *Remote Sensing*, vol. 11, no. 14, Art. no. 14, Jan. 2019, doi: 10.3390/rs11141650.

[81] G. Wenxia, S. Huanfeng, Z. Liangpei, and G. Wei, "Normalization of NDVI from Different Sensor System using MODIS Products as Reference," *IOP Conf. Ser.: Earth Environ. Sci.*, vol. 17, p. 012225, Mar. 2014, doi: 10.1088/1755-1315/17/1/012225.

[82] H. K. Zhang *et al.*, "Characterization of Sentinel-2A and Landsat-8 top of atmosphere, surface, and nadir BRDF adjusted reflectance and NDVI differences," *Remote Sensing of Environment*, vol. 215, pp. 482–494, Sep. 2018, doi: 10.1016/j.rse.2018.04.031.

[83] D. P. Roy *et al.*, "A general method to normalize Landsat reflectance data to nadir BRDF adjusted reflectance," *Remote Sensing of Environment*, vol. 176, pp. 255–271, Apr. 2016, doi: 10.1016/j.rse.2016.01.023.

[84] B. Franch *et al.*, "Toward Landsat and Sentinel-2 BRDF Normalization and Albedo Estimation: A Case Study in the Peruvian Amazon Forest," *Frontiers in Earth Science*, vol. 6, 2018, Accessed: Jun. 27, 2022. [Online]. Available: https://www.frontiersin.org/article/10.3389/feart.2018.00185

[85] J. R. Nagol, E. F. Vermote, and S. D. Prince, "Effects of atmospheric variation on AVHRR NDVI data," *Remote Sensing of Environment*, vol. 113, no. 2, pp. 392–397, Feb. 2009, doi: 10.1016/j.rse.2008.10.007.

[86] Y. Ke, J. Im, J. Lee, H. Gong, and Y. Ryu, "Characteristics of Landsat 8 OLI-derived NDVI by comparison with multiple satellite sensors and in-situ observations," *Remote Sensing of Environment*, vol. 164, pp. 298–313, Jul. 2015, doi: 10.1016/j.rse.2015.04.004.

[87] S. Liang, "Topographic Correction Methods," in *Quantitative Remote Sensing of Land Surfaces*, John Wiley & Sons, Ltd, 2003, pp. 231–245. doi: 10.1002/047172372X.ch7.

[88] J. Buchner *et al.*, "Land-cover change in the Caucasus Mountains since 1987 based on the topographic correction of multi-temporal Landsat composites," *Remote Sensing of Environment*, vol. 248, p. 111967, Oct. 2020, doi: 10.1016/j.rse.2020.111967.

[89] F. Li *et al.*, "A physics-based atmospheric and BRDF correction for Landsat data over mountainous terrain," *Remote Sensing of Environment*, vol. 124, pp. 756–770, Sep. 2012, doi: 10.1016/j.rse.2012.06.018.

[90] R. Fensholt and S. R. Proud, "Evaluation of Earth Observation based global long term vegetation trends — Comparing GIMMS and MODIS global NDVI time series," *Remote Sensing of Environment*, vol. 119, pp. 131–147, Apr. 2012, doi: 10.1016/j.rse.2011.12.015.

[91] T. Wang, "Vegetation NDVI Change and Its Relationship with Climate Change and Human Activities in Yulin, Shaanxi Province of China," *Journal of Geoscience and Environment Protection*, vol. 4, no. 10, Art. no. 10, Oct. 2016, doi: 10.4236/gep.2016.410002.

[92] M. K. Patasaraiya, B. Sinha, J. Bisaria, S. Saran, and R. K. Jaiswal, "ASSESSING IMPACTS OF CLIMATE CHANGE ON TEAK AND SAL LANDSCAPE USING MODIS TIME SERIES DATA," in *The International Archives of the Photogrammetry, Remote Sensing and Spatial Information Sciences*, Nov. 2018, vol. XLII–5, pp. 305–313. doi: 10.5194/isprs-archives-XLII-5-305-2018.

[93] X. Liu, Z. Tian, A. Zhang, A. Zhao, and H. Liu, "Impacts of Climate on Spatiotemporal Variations in Vegetation NDVI from 1982–2015 in Inner Mongolia, China," *Sustainability*, vol. 11, no. 3, Art. no. 3, Jan. 2019, doi: 10.3390/su11030768.

[94] L. Zhong, Y. Ma, Mhd. S. Salama, and Z. Su, "Assessment of vegetation dynamics and their response to variations in precipitation and temperature in the Tibetan Plateau," *Climatic Change*, vol. 103, no. 3, pp. 519–535, Dec. 2010, doi: 10.1007/s10584-009-9787-8.

[95] Ç. Sağır, M. Coz, B. Kurtulus, and M. Razack, *Determining climate change effects on vegetation in various land covers using NDVI in the Poitou region, France*. 2017.

[96] Y. Wen, X. Liu, F. Pei, X. Li, and G. Du, "Non-uniform time-lag effects of terrestrial vegetation responses to asymmetric warming," *Agricultural and Forest Meteorology*, vol. 252, pp. 130–143, Apr. 2018, doi: 10.1016/j.agrformet.2018.01.016.

[97] Y. Wen, X. Liu, J. Yang, K. Lin, and G. Du, "NDVI indicated inter-seasonal non-uniform time-lag responses of terrestrial vegetation growth to daily maximum and minimum temperature," *Global and Planetary Change*, vol. 177, pp. 27–38, Jun. 2019, doi: 10.1016/j.gloplacha.2019.03.010.

[98] Y. Ding, Z. Li, and S. Peng, "Global analysis of time-lag and -accumulation effects of climate on vegetation growth," *International Journal of Applied Earth Observation and Geoinformation*, vol. 92, p. 102179, Oct. 2020, doi: 10.1016/j.jag.2020.102179.

[99] D. Kong, C. Miao, J. Wu, H. Zheng, and S. Wu, "Time lag of vegetation growth on the Loess Plateau in response to climate factors: Estimation, distribution, and influence," *Science of The Total Environment*, vol. 744, p. 140726, Nov. 2020, doi: 10.1016/j.scitotenv.2020.140726.

[100] Y. Song and M. Ma, "A statistical analysis of the relationship between climatic factors and the Normalized Difference Vegetation Index in China," *International Journal of Remote Sensing*, vol. 32, no. 14, pp. 3947–3965, Jul. 2011, doi: 10.1080/01431161003801336.

[101] Z. Gu, X. Duan, Y. Shi, Y. Li, and X. Pan, "Spatiotemporal variation in vegetation coverage and its response to climatic factors in the Red River Basin, China," *Ecological Indicators*, vol. 93, pp. 54–64, Oct. 2018, doi: 10.1016/j.ecolind.2018.04.033.

[102] J. Sun and X. Qin, "Precipitation and temperature regulate the seasonal changes of NDVI across the Tibetan Plateau," *Environ Earth Sci*, vol. 75, no. 4, p. 291, Feb. 2016, doi: 10.1007/s12665-015-5177-x.

[103] H. Shen, L. Huang, L. Zhang, P. Wu, and C. Zeng, "Long-term and fine-scale satellite monitoring of the urban heat island effect by the fusion of multi-temporal and multi-sensor remote sensed data: A 26-year case study of the city of Wuhan in China," *Remote Sensing of Environment*, vol. 172, pp. 109–125, Jan. 2016, doi: 10.1016/j.rse.2015.11.005.

[104] X. W. Chuai, X. J. Huang, W. J. Wang, and G. Bao, "NDVI, temperature and precipitation changes and their relationships with different vegetation types during 1998–2007 in Inner Mongolia, China," *International Journal of Climatology*, vol. 33, no. 7, pp. 1696–1706, 2013, doi: 10.1002/joc.3543.

[105] B. Li, S. Tao, and R. W. Dawson, "Relations between AVHRR NDVI and ecoclimatic parameters in China," *International Journal of Remote Sensing*, vol. 23, no. 5, pp. 989–999, Jan. 2002, doi: 10.1080/014311602753474192.

[106] L. Cui and J. Shi, "Temporal and spatial response of vegetation NDVI to temperature and precipitation in eastern China," *J. Geogr. Sci.*, vol. 20, no. 2, pp. 163–176, Apr. 2010, doi: 10.1007/s11442-010-0163-4.

[107] F. Yunfei *et al.*, "Livestock Dynamic Responses to Climate Change in Alpine Grasslands on the Northern Tibetan Plateau: Forage Consumption and Time-Lag Effects," *jore*, vol. 8, no. 1, pp. 88–96, Jan. 2017, doi: 10.5814/j.issn.1674-764x.2017.01.011.

[108] A. S. Chartchyan, "The analyze of meteorological data and possible scenarios of climate change in Armenia.," *Armenia Climate Change Problems Collected Articles. Gitutyan, Yerevan*, pp. 33–49, 1999.

[109] H. S. Galstyan, "Trend detection in annual temperature using the mann-kendall test (case study: Meghri meteorological station of republic of Armenia).," *Hydrology, Meteorology and Climatology Issues in Armenia. Yerevan*, pp. 28–30, 2014.

[110] "Third National Communication on Climate Change: under the United Nations Framework Convention on Climate Change. Yerevan.," 2015.

[111] A. Aleksanyan, T. Aleksanyan, and G. Fayvush, "Modeling of rare ecosystems under climate change : as a tool for biodiversity conservation.," Biol. J. Armen. 68, 2016.

[112] J. J. Bellamy, "FINAL EVALUATION of the UNDP-Supported, GEF-Financed Project 'Adaptation to Climate Change Impacts in Mountain Forest Ecosystems of Armenia,'" 2013.

[113] A. Ziroyan, "Ecological-energetic Assessment of Vegetation of Armenia. Lusabac, Yerevan," 2008. https://scholar.google.com/scholar_lookup?title=Ecological-energetic%20Assessment%20of%20Vegetation%20of%20Armenia&author=A.%20Ziroyan&publication_year=2008 (accessed Jul. 08, 2022).

[114] C. Basnou, J. Pino, and S. Petr, "Effect of grazing on grasslands in theWestern Romanian Carpathians depends on the bedrock type," *Preslia*, vol. 81, Jun. 2009.

[115] C. A. Shisanya, C. Recha, and A. Anyamba, "Rainfall Variability and Its Impact on Normalized Difference Vegetation Index in Arid and Semi-Arid Lands of Kenya," *International Journal of Geosciences*, vol. 2, no. 1, Art. no. 1, Feb. 2011, doi: 10.4236/ijg.2011.21004.

[116] J. M. Suttie, S. G. Reynolds, and C. Batello, *Grassland of the world*. Rome, Italy: FAO, 2005. Accessed: Jun. 27, 2022. [Online]. Available: https://www.fao.org/publications/card/en/c/71c9e309-7d69-57c1-8915-f159643349ee/

[117] I. Ali, F. Cawkwell, E. Dwyer, B. Barrett, and S. Green, "Satellite remote sensing of grasslands: from observation to management," *Journal of Plant Ecology*, vol. 9, no. 6, pp. 649–671, Dec. 2016, doi: 10.1093/jpe/rtw005.

[118] A. Morán-Ordóñez, S. Suárez-Seoane, L. Calvo, and E. de Luis, "Using predictive models as a spatially explicit support tool for managing cultural landscapes," *Applied Geography*, vol. 31, no. 2, pp. 839–848, Apr. 2011, doi: 10.1016/j.apgeog.2010.09.002.

[119] W. Zhou *et al.*, "Grassland degradation remote sensing monitoring and driving factors quantitative assessment in China from 1982 to 2010," *Ecological Indicators*, vol. 83, pp. 303–313, Dec. 2017, doi: 10.1016/j.ecolind.2017.08.019.

[120] R. J. Scholes *et al.*, *IPBES (2018): Summary for policymakers of the assessment report on land degradation and restoration of the Intergovernmental Science- Policy Platform on Biodiversity and Ecosystem Services*. Intergovernmental Science-Policy Platform on Biodiversity and Ecosystem Services, 2018. Accessed: Jul. 11, 2022. [Online]. Available: https://research.utwente.nl/en/publications/ipbes-2018-summary-for-policymakers-of-the-assessment-report-

on-l

[121] K. E. Lewińska, P. Hostert, J. Buchner, B. Bleyhl, and V. C. Radeloff, "Short-term vegetation loss versus decadal degradation of grasslands in the Caucasus based on Cumulative Endmember Fractions," *Remote Sensing of Environment*, vol. 248, p. 111969, Oct. 2020, doi: 10.1016/j.rse.2020.111969.

[122] N. Gorelick, M. Hancher, M. Dixon, S. Ilyushchenko, D. Thau, and R. Moore, "Google Earth Engine: Planetary-scale geospatial analysis for everyone," *Remote Sensing of Environment*, vol. 202, pp. 18–27, Dec. 2017, doi: 10.1016/j.rse.2017.06.031.

[123] J. N. Schmid, "Using Google Earth Engine for Landsat NDVI time series analysis to indicate the present status of forest stands," 2017. doi: 10.13140/RG.2.2.34134.14402/6.

[124] A. B. Baghdasaryan, Institute of Geological Sciences, Department of Geography, and ASSR AS, Eds., *Physical geography of the Armenian SSR*. Yerevan: ASSR, AS, 1971.

[125] V. S. Muradyan and Sh. G. Asmaryan, "Applying landscape-ecological concept and GIS modelling for assessing and mapping of ecological situation of mountainous landscapes (on the case of Syunik marz, Armenia)," *Geocarto International*, vol. 30, no. 10, pp. 1077–1091, Nov. 2015, doi: 10.1080/10106049.2015.1013065.

[126] C. Wu *et al.*, "Remotely sensed estimation and mapping of soil moisture by eliminating the effect of vegetation cover," *Journal of Integrative Agriculture*, vol. 18, no. 2, pp. 316–327, Feb. 2019, doi: 10.1016/S2095-3119(18)61988-4.

[127] Z. Wang, C. B. Schaaf, Q. Sun, Y. Shuai, and M. O. Román, "Capturing rapid land surface dynamics with Collection V006 MODIS BRDF/NBAR/Albedo (MCD43) products," *Remote Sensing of Environment*, vol. 207, pp. 50–64, Mar. 2018, doi: 10.1016/j.rse.2018.02.001.

[128] C. E. Holden and C. E. Woodcock, "An analysis of Landsat 7 and Landsat 8 underflight data and the implications for time series investigations," *Remote Sensing of Environment*, vol. 185, pp. 16–36, Nov. 2016, doi: 10.1016/j.rse.2016.02.052.

[129] D. P. Roy *et al.*, "Characterization of Landsat-7 to Landsat-8 reflective wavelength and normalized difference vegetation index continuity," *Remote Sensing of Environment*, vol. 185, pp. 57–70, Nov. 2016, doi: 10.1016/j.rse.2015.12.024.

[130] D. Xu and X. Guo, "Compare NDVI Extracted from Landsat 8 Imagery with that from Landsat 7 Imagery," *American Journal of Remote Sensing*, vol. 2, no. 2, Art. no. 2, Sep. 2014, doi: 10.11648/j.ajrs.20140202.11.

[131] P. Li, L. Jiang, and Z. Feng, "Cross-Comparison of Vegetation Indices Derived from Landsat-7 Enhanced Thematic Mapper Plus (ETM+) and Landsat-8 Operational Land Imager (OLI) Sensors," *Remote Sensing*, vol. 6, no. 1, Art. no. 1, Jan. 2014, doi: 10.3390/rs6010310.

[132] E. Vermote, C. Justice, M. Claverie, and B. Franch, "Preliminary analysis of the performance of the Landsat 8/OLI land surface reflectance product," *Remote Sensing of Environment*, vol. 185, pp. 46–56, Nov. 2016, doi: 10.1016/j.rse.2016.04.008.

[133] S. Foga *et al.*, "Cloud detection algorithm comparison and validation for operational Landsat data products," *Remote Sensing of Environment*, vol. 194, pp. 379–390, Jun. 2017, doi: 10.1016/j.rse.2017.03.026.

[134] J. Colby, "Topographic normalization in rugged terrain," *Photogrammetric Engineering and Remote Sensing*, vol. 57, pp. 531–537, Apr. 1991.

[135] S. Vanonckelen, S. Lhermitte, and A. Van Rompaey, "The effect of atmospheric and topographic correction methods on land cover classification accuracy," *International Journal of Applied Earth Observation and Geoinformation*, vol. 24, pp. 9–21, Oct. 2013, doi: 10.1016/j.jag.2013.02.003.

[136] M. D. Nguyen, O. M. Baez-Villanueva, D. D. Bui, P. T. Nguyen, and L. Ribbe, "Harmonization of Landsat and Sentinel 2 for Crop Monitoring in Drought Prone Areas: Case Studies of Ninh Thuan (Vietnam) and Bekaa (Lebanon)," *Remote Sensing*, vol. 12, no. 2, Art. no. 2, Jan. 2020, doi: 10.3390/rs12020281.

[137] A. Poortinga *et al.*, "Mapping Plantations in Myanmar by Fusing Landsat-8, Sentinel-2 and Sentinel-1 Data along with Systematic Error Quantification," *Remote Sensing*, vol. 11, no. 7, Art. no. 7, Jan. 2019, doi: 10.3390/rs11070831.

[138] S. A. Soenen, D. R. Peddle, and C. A. Coburn, "SCS+C: a modified Sun-canopy-sensor topographic correction in forested terrain," *IEEE Transactions on Geoscience and Remote Sensing*, vol. 43, no. 9, pp. 2148–2159, Sep. 2005, doi: 10.1109/TGRS.2005.852480.

[139] M. Claverie *et al.*, "The Harmonized Landsat and Sentinel-2 surface reflectance data set," *Remote Sensing of Environment*, vol. 219, pp. 145–161, Dec. 2018, doi: 10.1016/j.rse.2018.09.002.

[140] D. P. Roy, Z. Li, H. K. Zhang, and H. Huang, "A conterminous United States analysis of the impact of Landsat 5 orbit drift on the temporal consistency of Landsat 5 Thematic Mapper data," *Remote Sensing of Environment*, vol. 240, p. 111701, Apr. 2020, doi: 10.1016/j.rse.2020.111701.

[141] F. Gao, T. He, J. G. Masek, Y. Shuai, C. B. Schaaf, and Z. Wang, "Angular Effects and Correction for Medium Resolution Sensors to Support Crop Monitoring," *IEEE Journal of Selected Topics in Applied Earth Observations and Remote Sensing*, vol. 7, no. 11, pp. 4480–4489, Nov. 2014, doi: 10.1109/JSTARS.2014.2343592.

[142] E. F. Vermote *et al.*, "Atmospheric correction of visible to middle-infrared EOS-MODIS data over land surfaces: Background, operational algorithm and validation," *Journal of Geophysical Research: Atmospheres*, vol. 102, no. D14, pp. 17131–17141, 1997, doi: 10.1029/97JD00201.

[143] Y.-L. Sun, M. Shan, X.-R. Pei, X.-K. Zhang, and Y.-L. Yang, "Assessment of the impacts of climate change and human activities on vegetation cover change in the Haihe River basin, China," *Physics and Chemistry of the Earth, Parts A/B/C*, vol. 115, p. 102834, Feb. 2020, doi: 10.1016/j.pce.2019.102834.

[144] Q. Yang *et al.*, "Assessing climate impact on forest cover in areas undergoing substantial land cover change using Landsat imagery," *Science of The Total Environment*, vol. 659, pp. 732–745, Apr. 2019, doi: 10.1016/j.scitotenv.2018.12.290.

[145] J. Gao, M. W. Williams, X. Fu, G. Wang, and T. Gong, "Spatiotemporal distribution of snow in eastern Tibet and the response to climate change," *Remote Sensing of Environment*, vol. 121, pp. 1–9, Jun. 2012, doi: 10.1016/j.rse.2012.01.006.

[146] H. B. Mann, "Nonparametric Tests Against Trend," *Econometrica*, vol. 13, no. 3, pp. 245–259, 1945, doi: 10.2307/1907187.

[147] M. G. Kendall, *Rank correlation methods*. London: Griffin, 1975.

[148] K. H. Hamed and A. Ramachandra Rao, "A modified Mann-Kendall trend test for autocorrelated data," *Journal of Hydrology*, vol. 204, no. 1, pp. 182–196, Jan. 1998, doi: 10.1016/S0022-1694(97)00125-X.

[149] P. K. Sen, "Estimates of the Regression Coefficient Based on Kendall's Tau," *Journal of the American Statistical Association*, vol. 63, no. 324, pp. 1379–1389, Dec. 1968, doi: 10.1080/01621459.1968.10480934.

[150] O. Gilbert, "Statistical Methods for Environmental Pollution Monitoring | Wiley," *Wiley.com*, 1987. https://www.wiley.com/en-us/Statistical+Methods+for+Environmental+Pollution+Monitoring-p-9780471288787 (accessed Jul. 11, 2022).

[151] M. M. Hussain and I. Mahmud, "pyMannKendall: a python package for non parametric Mann Kendall family of trend tests.," *Journal of Open Source Software*, vol. 4, no. 39, p. 1556, Jul. 2019, doi: 10.21105/joss.01556.

[152] S. Yue and C. Wang, "The Mann-Kendall Test Modified by Effective Sample Size to Detect Trend in Serially Correlated Hydrological Series," *Water Resources Management*, vol. 18, no. 3, pp. 201–218, Jun. 2004, doi: 10.1023/B:WARM.0000043140.61082.60.

[153] S. Yue, P. Pilon, B. Phinney, and G. Cavadias, "The influence of autocorrelation on the ability to detect trend in hydrological series," *Hydrological Processes*, vol. 16, no. 9, pp. 1807–1829, 2002, doi: 10.1002/hyp.1095.

[154] F. Serinaldi and C. G. Kilsby, "[논문]The importance of prewhitening in change point analysis under persistence," *Stochastic environmental research and risk assessment : research journal*, vol. 30, no. 2, pp. 763–777, 2016,

doi: 10.1007/s00477-015-1041-5.

[155] H. V. Storch, "Misuses of Statistical Analysis in Climate Research," in *Analysis of Climate Variability*, H. V. Storch and A. Navarra, Eds. Berlin, Heidelberg: Springer Berlin Heidelberg, 1995, pp. 11–26. doi: 10.1007/978-3-662-03167-4_2.

[156] P. S. Kaspersen, R. Fensholt, and S. Huber, "A Spatiotemporal Analysis of Climatic Drivers for Observed Changes in Sahelian Vegetation Productivity (1982–2007)," *International Journal of Geophysics*, vol. 2011, p. e715321, Dec. 2011, doi: 10.1155/2011/715321.

[157] Z. Liu, H. Wang, N. Li, J. Zhu, Z. Pan, and F. Qin, "Spatial and Temporal Characteristics and Driving Forces of Vegetation Changes in the Huaihe River Basin from 2003 to 2018," *Sustainability*, vol. 12, no. 6, Art. no. 6, Jan. 2020, doi: 10.3390/su12062198.

[158] R. Prăvălie, G. Bandoc, C. Patriche, and T. Sternberg, "Recent changes in global drylands: Evidences from two major aridity databases," *CATENA*, vol. 178, pp. 209–231, Jul. 2019, doi: 10.1016/j.catena.2019.03.016.

[159] R. Prăvălie *et al.*, "NDVI-based ecological dynamics of forest vegetation and its relationship to climate change in Romania during 1987–2018," *Ecological Indicators*, vol. 136, p. 108629, Mar. 2022, doi: 10.1016/j.ecolind.2022.108629.

[160] N. Linscheid *et al.*, "Towards a global understanding of vegetation–climate dynamics at multiple timescales," *Biogeosciences*, vol. 17, no. 4, pp. 945–962, Feb. 2020, doi: 10.5194/bg-17-945-2020.

[161] S. Weishou, J. Di, Z. Hui, Y. Shouguang, L. Haidong, and L. Naifeng, "The Response Relation between Climate Change and NDVI over the Qinghai-Tibet plateau," *International Journal of Environmental and Ecological Engineering*, vol. 5, no. 11, pp. 761–767, Nov. 2011.

[162] P. Zhang, B. Anderson, B. Tan, D. Huang, and R. Myneni, "Potential monitoring of crop production using a satellite-based Climate-Variability Impact Index," *Agricultural and Forest Meteorology*, vol. 132, no. 3, pp. 344–358, Oct. 2005, doi: 10.1016/j.agrformet.2005.09.004.

[163] B. Chen *et al.*, "Changes in vegetation photosynthetic activity trends across the Asia–Pacific region over the last three decades," *Remote Sensing of Environment*, vol. 144, pp. 28–41, Mar. 2014, doi: 10.1016/j.rse.2013.12.018.

[164] S. Piao, A. Mohammat, J. Fang, Q. Cai, and J. Feng, "NDVI-based increase in growth of temperate grasslands and its responses to climate changes in China," *Global Environmental Change*, vol. 16, no. 4, pp. 340–348, Oct. 2006, doi: 10.1016/j.gloenvcha.2006.02.002.

[165] T. Suepa, J. Qi, S. Lawawirojwong, and J. P. Messina, "Understanding spatio-temporal variation of vegetation phenology and rainfall seasonality in the monsoon Southeast Asia," *Environmental Research*, vol. 147, pp. 621–629, May 2016, doi: 10.1016/j.envres.2016.02.005.

[166] T. G. Workie and H. J. Debella, "Climate change and its effects on vegetation phenology across ecoregions of Ethiopia," *Global Ecology and Conservation*, vol. 13, p. e00366, Jan. 2018, doi: 10.1016/j.gecco.2017.e00366.

[167] J. Wang, P. Rich, and K. Price, "Temporal responses of NDVI to precipitation and temperature in the central Great Plains, USA. International Journal of Remote Sensing," *International Journal of Remote Sensing*, vol. 24, pp. 2345–2364, Jun. 2003, doi: 10.1080/01431160210154812.

[168] Z. Xin, J. Xu, and W. Zheng, "Spatiotemporal variations of vegetation cover on the Chinese Loess Plateau (1981–2006): Impacts of climate changes and human activities," *Sci. China Ser. D-Earth Sci.*, vol. 51, no. 1, pp. 67–78, Jan. 2008, doi: 10.1007/s11430-007-0137-2.

[169] D. S. Ragatoa, K. O. Ogunjobi, A. A. Okhimamhe, S. D. Francis, and L. Adet, "A Trend Analysis of Temperature in Selected Stations in Nigeria Using Three Different Approaches," *Open Access Library Journal*, vol. 5, no. 2, Art. no. 2, Feb. 2018, doi: 10.4236/oalib.1104371.

[170] S. K. Patakamuri, K. Muthiah, and V. Sridhar, "Long-Term Homogeneity, Trend, and Change-Point Analysis of Rainfall in the Arid District of Ananthapuramu, Andhra Pradesh State, India," *Water*, vol. 12, no. 1, Art. no. 1,

Jan. 2020, doi: 10.3390/w12010211.

[171] M. Shen, G. Zhang, N. Cong, S. Wang, W. Kong, and S. Piao, "Increasing altitudinal gradient of spring vegetation phenology during the last decade on the Qinghai–Tibetan Plateau," Agricultural and Forest Meteorology, vol. 189–190, pp. 71–80, Jun. 2014, doi: 10.1016/j.agrformet.2014.01.003.